National Park Service
U.S. Department of the Interior

Natural Resource Stewardship and Science

Developing Critical Loads of Nitrate and Sulfate Deposition to Watersheds of Great Smoky Mountains National Park, United States

Natural Resource Technical Report NPS/GRSM/NRTR—2014/896

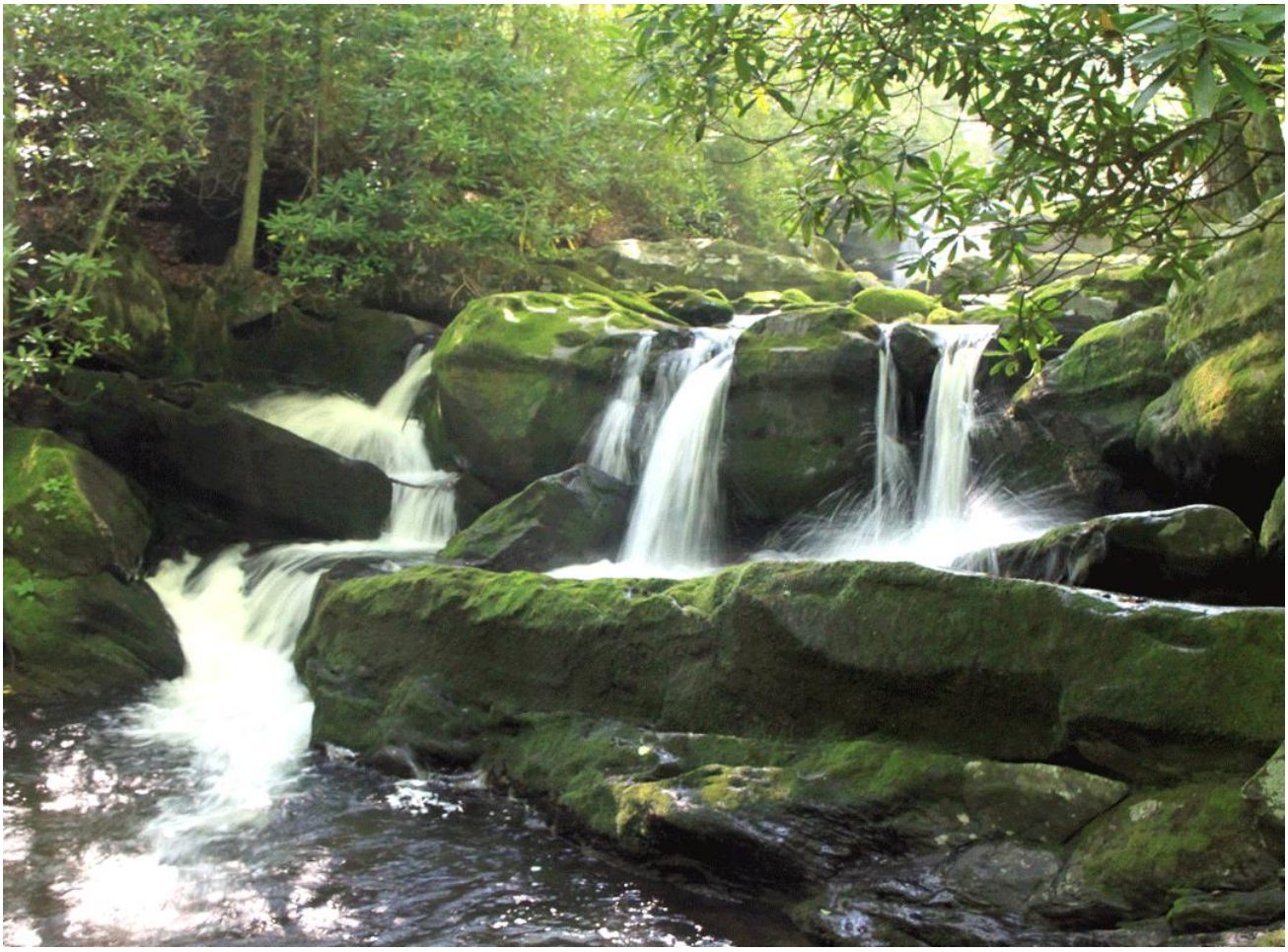

ON THE COVER
Photograph of Lynn Camp Prong in Great Smoky Mountains National Park
Image Courtesy of Jay Aldrich

Developing Critical Loads of Nitrate and Sulfate Deposition to Watersheds of Great Smoky Mountains National Park, United States

Natural Resource Technical Report NPS/GRSM/NRTR—2014/896

[1]Qingtao Zhou
[1]Charles T. Driscoll
[2]Stephen E. Moore
[2]Matt A. Kulp
[2]James R. Renfro
[3]John S. Schwartz
[3]Meijun Cai

[1]Department of Civil and Environmental Engineering
Syracuse University
Syracuse, NY 13244

[2]National Park Service
Great Smoky Mountains National Park
Gatlinburg, TN 37738

[3]Department of Civil and Environmental Engineering
University of Tennessee
Knoxville, TN 37996

August 2014

U.S. Department of the Interior
National Park Service
Natural Resource Stewardship and Science
Fort Collins, Colorado

The National Park Service, Natural Resource Stewardship and Science office in Fort Collins, Colorado, publishes a range of reports that address natural resource topics. These reports are of interest and applicability to a broad audience in the National Park Service and others in natural resource management, including scientists, conservation and environmental constituencies, and the public.

The Natural Resource Technical Report Series is used to disseminate results of scientific studies in the physical, biological, and social sciences for both the advancement of science and the achievement of the National Park Service mission. The series provides contributors with a forum for displaying comprehensive data that are often deleted from journals because of page limitations.

All manuscripts in the series receive the appropriate level of peer review to ensure that the information is scientifically credible, technically accurate, appropriately written for the intended audience, and designed and published in a professional manner.

This report received formal peer review by subject-matter experts who were not directly involved in the collection, analysis or reporting of the data, and whose background and expertise put them on par technically and scientifically with the authors of the information.

Views, statements, findings, conclusions, recommendations, and data in this report do not necessarily reflect views and policies of the National Park Service, U.S. Department of the Interior. Mention of trade names or commercial products does not constitute endorsement or recommendation for use by the U.S. Government.

This report is available in digital format from the Greater Smoky Mountains National Park website (http://www.nps.gov/grsm/index.htm) and the Natural Resource Publications Management website (http://www.nature.nps.gov/publications/nrpm/). To receive this report in a format optimized for screen readers, please email irma@nps.gov.

Please cite this publication as:

Zhou, Q., C. T. Driscoll, S. E. Moore, M. A. Kulp, J. R. Renfro, J. S. Schwartz, and M. Cai. 2014. Developing critical loads of nitrate and sulfate deposition to watersheds of the Great Smoky Mountains National Park, United States. Natural Resource Technical Report NPS/GRSM/NRTR—2014/896. National Park Service, Fort Collins, Colorado.

133/125667, August 2014

Contents

Page

1. Introduction 1

2. Methods 3

2.1. Sites 3

2.2. Data Sets 4

2.2.1. Meteorological Data 4

2.2.2. Atmospheric Deposition 4

2.2.3. Land Disturbance 7

2.2.4. Stream Data 7

2.2.5. Model Application and Evaluation 7

3. Results 9

3.1. Model Performance 9

3.2. Hindcasts (1850–2010) for Stream Chemistry at GRSM 13

3.3. Future Projections 14

3.4. Factors Affecting Historical Acidification and Recovery 17

3.5. Projections of DCLs 19

4. Discussion 21

4.1. Model Performance 21

4.2. Mass balances for Noland Divide Watershed and Goshen Prong Watershed 22

4.2.1. Mass Balance for Noland Divide Watershed 22

4.2.2. Element and ANC Budgets for Goshen Prong Watershed (GPW) 24

4.3. Comparison of controls on SO_4^{2-}, NO_3^- and NH_4^+deposition 28

4.4. Developing CLs/DCLs for GRSM 31

5. Conclusions 35

6. Literature Cited 37

Figures

Page

Figure 1. Model comparison between measured and model-predicted mean annual volume-weighted concentrations of selected stream solutes for 12 sites in GRSM 10

Figure 2. Simulations of hindcasts of SO_4^{2-}, NO_3^-, and acid neutralizing capacity (ANC) for stream chemistry sites in GRSM. 14

Figure 3. Time series of stream SO_4^{2-}, NO_3^-, Ca^{2+}, ANC and pH for Goshen Prong watershed (y-axis) that include hindcasts and future projections to atmospheric deposition decreases in: (a) NO_3^- only, (b) SO_4^{2-} only, and (c) both NO_3^- and SO_4^{2-}. 16

Figure 4. Relationships between (a) preindustrial ANC(1850); (b) current total deposition of SO42- +NO3- ; and (c) estimated soil sulfate adsorption capacity with historical acidification HA; ANC in 1850 – ANC in 2010). 18

Figure 5. Empirical relationships between current ANC of GRSM streams and the deposition of NO3- + SO42- necessary to achieve target ANC values of 0, 20 and 50 µeq/L in 2050. 20

Figure 6. Isopleth map of combinations of total SO42- and NO3- deposition for Noland Divide Watershed that result in a value of ANC. 30

Tables

Page

Table 1. Characteristics of watersheds from GRSM that are used to test and apply PnET-BGC. 3

Table 2. Regression equations for mean monthly precipitation quantity based on longitude, latitude, and elevation in GRSM. 6

Table 3. Regression equations for mean quarterly SO_4^{2-} and NO_3^- concentrations in wet deposition dependent on longitude, latitude, and elevation at GRSM. 6

Table 4. Summary of the results of model simulations of mean annual volume-weighted concentrations for selected stream solutes for 12 sites in GRSM. 11

Table 5. Available measurements and model simulations of element fluxes for Noland Divide Watershed. UT measured values are mean annual values for 1994–2008. IFS measurements were made during 1986–1989. 24

Table 6. Element and ANC budgets for Goshen Prong Watershed for preindustrial (1850–1860) and current (1999–2009) periods. 26

Table 7. Element and ANC budgets for hypothetical recovery of Goshen Prong Watershed. 27

Table 8. Changes in stream acid neutralizing capacity per unit equivalent decrease in ammonium and nitrate deposition for watersheds of Great Smoky Mountain National Park over the period to 2050. 30

Table 9. Dynamic critical loads (DCL) of NO3- + SO42 deposition necessary to reach ANC targets at various time steps based upon PnET-BGC model forecasts for 12 study stream within Great Smoky Mountains National Park. 33

Table 10. Projected streamwater ANC for twelve GRSM modeled watersheds under pre-industry time; Streamwater ANC, pH under current deposition scenario compared with streamwater pH, ANC in 2040 under 60% reduction scenario 34

Appendices

Page

Appendix 1: Time Series of Stream 41

Abstract

Long-term impacts of acidic deposition on Great Smoky Mountains National Park include elevated inputs of sulfate and nitrate, the depletion of available base cations from soil, acidification of high elevation streams and extirpation of trout. Critical Loads and dynamic critical loads (CLs/DCLs) are useful tools to evaluate ecosystem response to controls on acidic deposition and help guide future air quality management. We evaluate the application of CLs/DCLs of nitrate and sulfate deposition for 12 watersheds in Great Smoky Mountains National Park (GRSM), USA using the hydrochemical model, PnET-BGC. Twelve sites were chosen for model application based on a block design to represent characteristics of the entire Park. Two of the streams studied are listed by the state of Tennessee as impaired due to low stream pH, and have acid neutralizing capacity (ANC) ranging from -14 μeq/L – 60 μeq/L. We reconstructed historical meteorological, atmospheric deposition and land disturbance data for study watersheds for the period 1850 to present for model hindcasts. As future emissions are expected to decline, the model was run under a range of future scenarios from 2008 to 2200 of decreases in sulfate, nitrate and ammonium, and combinations of sulfate and nitrate deposition to estimate CLs and DCLs to evaluate how watersheds might respond to emission control strategies. Model simulations of stream chemistry generally agreed with long-term (>10 yr.) observations. Results of model simulations also compare favorably with biogeochemical data from the long-term study watershed, Noland Divide Watershed. Model simulations suggest that stream response to historic atmospheric sulfate deposition is in part controlled by soil sulfate adsorption and mobilization of base cations from soil exchange pools. Retention of atmospheric nitrogen deposition is limited in some watersheds resulting in elevated leaching losses of nitrate. Model hindcasts indicate that watersheds in GRSM are inherently sensitive to acidic deposition. Simulated mean stream ANC of 71 μeq/L (range 32 μeq/L – 107 μeq/L) prior to industrial development (~1850) decreases in response historical acidic deposition to 33 μeq/L (-13 μeq/L – 88 μeq/L) in 2007. Historical acidification of GRSM exhibited a similar long-term temporal pattern across the watersheds. Future model projections for GRSM show that decreases in sulfate deposition result in smaller increases in stream ANC compared with equivalent decreases in nitrate deposition. Although there are no programs in the U.S. to control ammonia emissions, model simulations suggest that decreases in ammonium deposition could also help mitigate acidification to a comparable of greater extent than equivalent controls on nitrate deposition. The timescale of watershed recovery to decreases in acidic deposition is multiple decades to centuries. Increases in soil pH associated with decreases in atmospheric nitrate deposition results in desorption of sulfate from soil to drainage water, delaying watershed recovery for decades from acidic deposition. Simulations suggest that simultaneous reductions of nitrate and sulfate deposition are essential to limit ongoing acidification to GRSM watersheds and they are more effective than individual reductions of nitrate or sulfate.

Acknowledgments

This work was supported by the National Park Service under Agreement H54710090015 signed September 25, 2009. The authors wish to thank Brendan Davison and Melanie Peters for all their hard work in editing the report.

Keywords

Acidic deposition, acidification modeling, critical loads, Great Smoky Mountains National Park, watersheds

1. Introduction

Great Smoky Mountains National Park (GRSM) is a 1,999 km^2 Class I Airshed in the Southern Appalachian Mountains of Tennessee and North Carolina, USA. GRSM receives high atmospheric sulfur (S) and nitrogen (N) deposition (Johnson and Lindberg, 1992). In 2000, total S deposition ranged from 7 to 42 kg S/ha-yr and total N deposition ranged from 5 to 31 kg N/ha-yr (Weathers et al., 2006). Air quality management, through the Clean Air Act and the U.S. Environmental Protection Agency NO_x Budget Trading Program and the Clean Air Interstate Rule (CAIR), among other programs, has resulted in decreases in atmospheric sulfate (SO_4^{2-}) and nitrate (NO_3^-) deposition in the eastern U.S. (Lehmann et al., 2005). Currently (2004-2008) atmospheric S and N deposition across GRSM range from 6.8 to 27.8 kg S/ha-yr and 6.1 to 16.6 kg N/ha-yr, respectively.

Watersheds of GRSM are sensitive to acidic deposition due to high elevation topographic features coupled with highly weathered, unglaciated, base-poor soils, shallow hydrologic flowpaths and mature forests (Johnson and Lindberg, 1992; Cai et al., 2012; Neff et al., 2013). Atmospheric S and N deposition have resulted in acidification of the soil and the stream water in GRSM (Nodvin et al., 1995; Robinson et al., 2008) and throughout the Southern, Central and Northern Appalachian Mountains (Kahl et al., 2004). Cai et al. (2010) investigated two streams in Noland Divide, a high elevation watershed in GRSM, showing that stream acidification was associated with elevated atmospheric SO_4^{2-}, NH_4^+ and NO_3^- deposition; precipitation quantity; high nitrification rates in A horizon soil; and adsorption of SO_4^{2-} and supply of base cations from soil. Soil SO_4^{2-} adsorption is a critical controller of soil and stream acidification (Cai et al., 2012). Soils from Noland Divide watershed are not at steady-state with respect to atmospheric SO_4^{2-} deposition; the watershed is retaining SO_4^{2-} inputs limiting transport to streams.

Section 303(d) of the Clean Water Act requires states to list waters for which technology-based effluent limitations are not adequate to meet water quality standards. In 2006, Tennessee listed 12 streams in GRSM, two of which are included in our research, as not supporting designated use classification (i.e., impaired) due to acidity, associated with pH values below 6.0 (Goshen Prong and Cannon Creek; TDEC 2010; Neff et al., 2009). The designated use classifications for streams in GRSM include protection of fish and aquatic life, wildlife and recreation. A total maximum daily load (TMDL) analysis for acid-impaired watersheds was conducted by the Tennessee Department of Environment and Conservation determining that the source of acidity was largely from regional atmospheric sources of acidic deposition.

A “critical load” (CL) is an estimate of deposition of one or more pollutants below which significant harmful effects on specified sensitive elements of the ecosystem do not occur according to present knowledge (Sullivan et al., 2012; Nilsson and Grennfelt, 1988; Burns et al., 2008). A related concept “target load” (TL) is the deposition of one or more pollutants that result in an acceptable level of resource protection based on policy, economic, or temporal considerations (Porter et al., 2005). CLs depict a steady-state condition of an ecosystem to a given level of atmospheric deposition. Dynamic Critical Loads (DCLs) are a type of target load representing dynamic conditions of an ecosystem that is not at steady-state with respect to acidic deposition, but changing over time. CLs can be

determined using steady-state or dynamic models (McNulty et al., 2007; Sullivan et al., 2012) or with empirical observations (Pardo, 2010). DCLs can only be characterized with dynamic models. CLs and DCLs are tools used by scientists, policy makers, and engineers to depict the inputs of air pollutants that an ecosystem can sustain without damage to its structure or function and to guide management decisions on ecosystem effects of air pollution. CLs have been developed and used by the National Park Service, including GRSM for terrestrial resources, to guide air quality management in Class I areas (Porter et al., 2005; Pardo et al., 2011; Baron et al., 2011).

The overall objective of this study was to apply and test the biogeochemical model PnET-BGC to 12 watersheds characteristic of GRSM, including two 303d listed streams, to ultimately establish CLs/DCLs for GRSM and evaluate stream water chemistry in response to decreases in acidic deposition. The specific objectives are to:

1. Compile data and apply the dynamic biogeochemical model (PnET-BGC) to test model simulations of hydrochemistry of watersheds in GRSM;

2. Simulate the response of different watersheds to historical increases in acidic deposition and project their responses to hypothetical decreases in atmospheric SO_4^{2-} NO_3^-, NH_4^+ deposition;

3. Evaluate the physical and biogeochemical factors that affect the response of GRSM watershed to changes in atmospheric SO_4^{2-}, NO_3^- and NH_4^+ deposition; and

4. Determine the CLs/DCLs of atmospheric SO_4^{2-} and NO_3^- deposition required to reach target ANCs (if possible) for various time periods.

2. Methods

Sites

We selected 12 watersheds for model application, ten of which represent a large proportion of the variability within GRSM based on stream water acid neutralizing capacity (ANC), elevation, watershed area, historical land disturbance, NO_3^- leaching, and the presence/absence of Anakeesta in the watershed (Neff et al., 2013; Table 1). Anakeesta is a sulfur bearing rock which can release SO_4^{2-} to drainage waters if the watershed is disturbed, for example from a rock slide or a road cut (Elwood et al., 1991). Two watersheds (Goshen Prong, Cannon Creek) were selected for model application because they contained streams on the Tennessee 303d list, indicating they do not meet water quality pH standards for intended use (i.e., mean stream pH>6.0) (TDEC, 2010). Noland Divide Watershed was selected for study because atmospheric deposition and stream chemistry have been monitored since 1991 by the University of Tennessee and there is an extensive data record from the Integrated Forest Study (1985–1989) and process studies by the University of Tennessee which were used for the validation of the model and assessment. Watershed areas for the 12 study sites range from 0.174 km^2 – 10.92 km^2; elevations range 545 m – 1,798 m and annual volume weighted NO_3^- concentrations range from 3.7 µeq/L – 56.1 µeq/L, indicating a diverse range of characteristics to facilitate model testing and application.

Table 1. Characteristics of watersheds from GRSM that are used to test and apply PnET-BGC. These values represent average between 1995–2006 except Noland Divided Watershed between 1994–2008.

Site	Elevation (m)	Area (km2)	%Anakeesta	NO3- (µeq/L)	SO42- (µeq/L)	ANC (µeq/L)	Impaired
Noland Divide	1798	0.174	No	44.3	40.9	4.3	
Indian Camp Creek	1205	2.17	No	42.1	57.0	17.8	
Walker Camp	1168	10.73	81.89%	38.0	71.2	-13.8	
Goshen Prong	1046	7.29	26.83%	21.2	30.3	20.8	303d
Lost Bottom	1000	5.15	No	7.7	16.5	50.3	
Left Prong Anthony	909	1.61	No	23.4	26.1	34.8	
Pretty Hollow	903	11.18	No	16.6	20.6	47.0	
Cosby Creek	783	5.78	No	38.2	46.1	37.3	
Sugar Fork	780	2.14	No	3.7	22.5	90.3	
Cannon Creek	751	4.19	0.64%	20.6	39.7	16.2	303d
Thunderhead	664	11.26	34.73%	14.4	31.2	33.2	
Mill Creek	545	10.92	No	12.1	24.8	46.2	

Data are from great Smoky Mountains National Park, National Park Service.

Data Sets

PnET-BGC was developed from the forest vegetation model, PnET-CN which simulates energy, water, carbon (C), and nitrogen (N) dynamics (Aber and Driscoll, 1997; Aber et al., 1997). PnET-BGC extends the simulations of PnET-CN to include the cycling of all major elements (i.e., C, N, P, S, Ca, Mg, K, Na, Al, Cl, Si). Both major biotic and abiotic processes are represented in PnET-BGC, including atmospheric deposition, canopy interaction, CO_2 fertilization, litterfall, forest growth, root uptake, snowpack accumulation and loss, soil organic matter dynamics, N mineralization and nitrification, mineral weathering, chemical reactions involving solid and solution phases, and surface water processes (Gbondo-Tugbawa et al., 2001).

PnET-BGC has been widely used in the northeastern U.S. It has been well validated in small watersheds with comprehensive field data for model testing (Gbondo-Tugbawa et al., 2001; Chen and Driscoll, 2004; Pourmokhtarian et al., 2012), but has also been applied at the regional scale (Chen and Driscoll, 2004; Chen and Driscoll, 2005; Zhai et al., 2008). This study is the first effort to apply the model to unglaciated watersheds in the southeastern U.S. PnET-BGC requires time series of meteorological data, atmospheric deposition, element weathering, overstory forest vegetation type and land-disturbance history as input data. In addition, site specific or regional forest type parameter values are used including vegetation stoichiometry, soil selectivity and adsorption coefficients, soil depth, bulk density and water holding capacity. The model was run on a monthly time step consistent with protocols used in similar long term simulations with results reported at defined yearly time steps (e.g., 2050, 2100, and 2200).

Meteorological Data

Meteorological data used to help drive model simulations include monthly minimum and maximum air temperatures, precipitation and solar radiation. Several meteorological datasets were used. For Noland Divide Watershed (35° 34' N, 83° 28' W; elev: 1,798m), meteorological data between 1993 and 2007 were obtained from Clingman's Dome (35° 32' 59"N, 83° 30' 0"W; elev: 2,003m), which is the highest peak in GRSM and a monitoring site from the National Park Service. Meteorological data for the period 1931 and 1993 were extrapolated using Waterville 2 coop station (35° 46' N, 83° 5' 59"W; EL: 439m) as a reference site. Meteorological data for Waterville 2 are available from 1931 to present (http://www.ncdc.noaa.gov). For hindcast simulations prior to 1931, monthly meteorological data were assumed to be constant at the mean of monthly values from 1931–1941. For forecast projections, temperatures and precipitation data are assumed to be constant as of the mean of monthly values from 1993–2007. Available solar radiation data (1993–2007) are from National Park Service Air Resources Division (http://ard-request.air-resource) Clingmans Dome air quality monitoring station. The mean values of solar radiation from 1993–2007 are used for hindcast and forecast simulations.

Atmospheric Deposition

Historical atmospheric deposition (1000 –1979) was reconstructed for the 12 watersheds in GRSM. The wet deposition data for major ions (Ca^{2+}, Mg^{2+}, K^{+}, Na^{+}, NO_3^{-}, SO_4^{2-}, Cl^{-}, NH_4^{+}) at Noland Divide watershed are available through the University of Tennessee. We developed a spatial relationship of precipitation quantity (Table 2) and precipitation chemistry (e.g., Table 3) for GRSM

using monthly data at five nearby monitoring sites (NC25, NC45, TN00, TN04, TN11) from the National Atmospheric Deposition Program (NADP). Empirical relationships for precipitation quantity and solute concentrations were developed using geographic position (latitude, longitude) and elevation (Table 2). As the product of precipitation quantity and solute concentrations, monthly wet deposition values were estimated for each of the study watersheds based on values that were scaled to wet deposition at Noland Divide watershed. This is similar to the approach used by Ollinger et al. (1993) and Ito et al. (2002) for the northeast U.S.

The historical wet deposition data from 1900 –1980 for use in hindcast simulations were estimated from the Advanced Statistical Trajectory Regional Air Pollution (ASTRAP) model (Shannon, 1981). The ASTRAP model was applied as part of the Southern Appalachian Mountain Initiative (SAMI) (Shannon, J.D. unpublished) to estimate historical deposition at five-year intervals, with results that are representative of a moving average centered about a particular year. For the preindustrial period (prior to 1850), we assume that the deposition was 10% of current deposition. The relative temporal pattern of historical deposition was assumed to be the same for each of the watersheds, with values scaled to deposition at Noland Divide watershed.

Total deposition for GRSM includes dry deposition (e.g., gaseous SO_2 and aerosol SO_4^{2-}), wet deposition (e.g., SO_4^{2-} from precipitation) and cloud deposition (e.g., cloud water or droplets containing SO_4^{2-}). To estimate dry deposition, we used dry to wet deposition ratios for major cations and anions. Throughfall monitoring data are available for coniferous vegetation at Noland Divide watershed through a routine monitoring program at the University of Tennessee (Cai et al., 2010) and at a hardwood stand from the Integrated Forest Study (Johnson and Lindberg, 1992). Throughfall deposition is the hydrologic flux of N and S from the forest canopy to the forest floor. It includes wet, dry and cloud deposition. Dry deposition is input that is not part of wet deposition, including deposition of gases and particles. We assumed that dry deposition of SO_4^{2-} and Cl^- can be calculated as the difference between throughfall and wet deposition. Dry to wet deposition ratios were prorated for the study watersheds from the distribution of hardwood and conifer forest cover for a given watershed. Dry to wet deposition ratios were assumed to be constant for the simulation period. Dry and cloud deposition represented approximately 70% for total SO_4^{2-} deposition and about 75% total NO_3^- deposition at the high elevation Noland Divided Watershed during 1986–1989 (Johnson and Lindberg, 1992).

Table 2. Regression equations for mean monthly precipitation quantity based on longitude, latitude, and elevation in GRSM.

	Constant (cm)	Longitude (cm/deg)	Latitude (cm/deg)	Elevation (cm/m)	Adj r^2	p
January	-198.232	-2.93	-1.02	0.00427	0.985	0.158
February	-304.497	-5.193	-3.331	0.004	0.987	0.146
March	-206.915	-4.482	-4.454	0.00676	0.978	0.187
April	-198.232	-2.93	-1.02	0.00427	0.938	0.158
May	-69.424	-2.178	-2.827	0.00378	0.541	0.791
June	355.77	2.311	-4.172	0.00151	0.935	0.321
July	287.745	3.431	0.377	-0.00091	0.275	0.933
August	508.106	5.403	-1.336	0.00148	0.997	0.073
September	-36.912	-2.851	-5.373	0.0041	0.99	0.129
October	62.165	-0.612	-3.016	0.00397	0.998	0.053
November	78.386	-0.973	-4.14	0.00292	0.995	0.092
December	72.583	-0.736	-3.438	0.000736	0.987	0.144

Table 3. Regression equations for mean quarterly SO_4^{2-} and NO_3^- concentrations in wet deposition dependent on longitude, latitude, and elevation at GRSM.

Quarter	Constant (*μeq/L*)	Longitude (*μeq/L-deg*)	Latitude (*μeq/L-deg*)	Elevation (*m*)	Adj.R^2	p
(a)						
Winter	-1.48×10^{3}	-1.68×10	2.45	1.03×10^{-2}	0.828	0.188
Spring	-1.82×10^{3}	-2.11×10	1.58	1.64×10^{-2}	0.974	0.102
Summer	-2.69×10^{3}	-3.19×10	0.80	2.79×10^{-2}	0.987	0.073
Autumn	-2.04×10^{3}	-2.39×10	1.38	2.04×10^{-2}	0.962	0.124
(b)						
Winter	-1.78×10^{3}	-1.83×10	7.44	1.06×10^{-2}	0.452	0.46
Spring	-1.46×10^{3}	-1.52×10	5.70	1.48×10^{-2}	0.875	0.224
Summer	-1.55×10^{3}	-1.57×10	7.56	1.41×10^{-2}	0.987	0.073
Autumn	-2.77×10^{3}	-3.10×10	5.07	2.64×10^{-2}	0.954	0.136

Land Disturbance

GRSM was established in 1934. Prior to that time more than one half of the total area of the Park had been cut by private logging companies (Pyle, 1985). Hurricanes, logging, farming and fire have affected and changed landscape patterns (Pyle, 1985). More recently, the infestation of exotic pests and air pollution have impacted the forests. The balsam woolly adelgid (BWA) has caused heavy mortality of *Abies balsamea*, killing virtually every individual fir tree less than 10 cm diameter at breast height (Moore et al., 2008). There were also three hurricanes in 1989, 1995 and 2004 that caused extensive forest damage (Moore et al., 2008). However, there is no record of the fraction of the study watersheds impacted by hurricane damage.

Historical land disturbance was estimated by digitizing National Park Service land disturbance records of the for the study watersheds. Land disturbance included historical logging, agricultural and settlement, fire, BWA damage (Smith and Nicholas, 2000), windstorms (White and Cogbill, 1992), and ice storms (Nicholas and Zedaker, 1989; Moore et al., 2008). Estimates of the fraction of the watershed impacted by disturbance and fraction of biomass removal were estimated based on archive records for GRSM.

Stream Data

Stream monitoring data for strong acid anions (NO_3^-, SO_4^{2-}, Cl^-), NH_4^+, ANC, and pH at Noland Divide are available from 1991–2008. Base cations data (Ca^{2+}, Mg^{2+}, Na^+, K^+) are available from 1993–2008. All of the data are biweekly based on the long-term monitoring program conducted by the University of Tennessee and the National Park Service (Robinson et al., 2008). Biweekly data of chemical species were converted to monthly volume-weighted concentrations and then converted into annual volume-weighted concentrations for comparison with simulation annual data. For the other eleven sites, stream water samples were collected on a monthly basis by GRSM staff from 1994–1996, quarterly 1997–2003, and bi-monthly from 2004–2008 (Schwartz et al., 2012). Monthly data from these sites were converted into annual volume-weighted concentrations. Stream discharge data are available for Noland Divide Watershed. GRSM stream water quality data and Noland Divide chemistry and discharge data are accessible via the EPA STORET data warehouse (http://www.epa.gov/storet/dw_home.html) using the "11NPSWRD" Organization ID.

Model Application and Evaluation

Following previous research (Zhai et al., 2008), model runs were started for individual GRSM watersheds in 1000 AD, and run under constant background deposition and no land disturbance until 1850 to achieve steady-state and evaluate "background" (i.e., pre 1850) conditions. Changes in atmospheric deposition and land disturbance events were initiated after 1850. The model was run from 1850–2010 based on measured values of atmospheric deposition and reconstructions of historical deposition from emission records. Model simulations continued through the year 2100 with a series of forecasts, which included a range of deposition scenarios from current to "background" deposition at 20% interval (0%, 20%, 40%, 60%, 80% and 100%) for SO_4^{2-} and NO_3^- individually and in combination. Future scenarios involved a 12 year linear decrease from 2008 values to the level of deposition of interest in 2020 and continued simulation at this deposition level until 2200. This range of deposition values was used to evaluate tradeoffs associated with reductions in SO_2 or NO_x emissions to achieve ecosystem recovery from acidic deposition.

This study also evaluated the degree to which decreases in NH_4^+ deposition influence the rate of watershed recovery from atmospheric deposition. As described above, we examined a range of future scenarios in which NH_4^+ deposition was incrementally decreased which were compared to the simulated response to incremental decreases in atmospheric NO_3^- deposition. These comparisons were conducted for four watersheds: one site, Lost Bottom Creek, which exhibits limited NO_3^- loss in streamwater and three sites which are characterized by elevated concentrations of NO_3^- in streamwater, Noland Divide, Walker Camp Prong and Indian Camp Creek.

We used normalized mean error (NME) and normalized mean absolute error (NMAE) methods (Janssen and Heuberger, 1995) to evaluate the agreement between model simulations with measurements of stream chemistry. These metrics can be obtained from equations as follows:

$$NME = \frac{\overline{p} - \overline{o}}{\overline{o}}; NMAE = \frac{\sum_{t=1}^{n} (|p_t - o_t|)}{n\overline{o}}$$

Where p_t is the predicted value at time t; o_t is the observed value at time t; $\overline{o}$ and $\overline{p}$ are the average observed and predicted values over time t; and n is the number of observations. NME represents the error between simulation results and observations. NMAE represents the absolute error between simulation results and observations. Negative values for NME mean that the prediction values are less than observation values. Positive values for NME mean that the prediction values are more than observation values.

3. Results

Model Performance

Generally PnET-BGC effectively simulated the hydrology and chemistry of stream waters at GRSM (Figure 1; Table 4). Measured annual discharge (1422 + 335 mm mean + SD) was similar to simulated values (1330 + 429 mm; NME -0.064, NMAE 0.11). For most stream solutes, model values were in agreement with simulated concentrations, with little bias for individual sites (simulated NME Mg^{2+} -0.13–0.17; Ca^{2+} -0.24–0.19; SO_4^{2-} -0.07–0.39; ANC -0.46–0.32; pH -0.04–0.07). While generally the agreement for Ca^{2+} was good, Indian Camp Creek (NME -0.24) and Cosby Creek (NME -0.24) sites with the Ca^{2+} highest concentrations were underpredicted. Model simulations did exhibit some bias for NO_3^- (NME -0.63–0.05). Stream NO_3^- is underpredicted compared to measured values particularly for Pretty Hollow (NME = -0.63), Sugar Fork (NME = -0.53), Cannon Creek (NME = -0.45) and Thunderhead (NME = -0.43). Watersheds where NO_3^- is overpredicted are generally at lower elevation and exhibit relatively low NO_3^- leaching (annual volume-weighted NO_3^- < 20 μeq/L). PnET-BGC simulated ANC (NME: -0.46–0.32) reasonably well, although simulations which underpredicted NO_3^- - tended to overpredict ANC.

In addition to stream monitoring data, biogeochemical process information is available for Noland Divide. Noland Divide watershed was the site of intensive research conducted from 1985–1989 through the Integrated Forest Study (IFS; Johnson and Lindberg, 1992) which experienced higher atmospheric deposition prior to the current monitoring program. More recently throughfall and drainage measurements have been made by the University of Tennessee (Cai et al., 2010). Mean annual mass balances and process fluxes for NH_4^+ (keq/ha-yr), NO_3^- (keq/ha-yr), SO_4^{2-} (keq/ha-yr) and Ca^{2+} (keq/ha-yr) are shown in Table 5 for measured values from the earlier IFS and more recently from the University of Tennessee (1991–2008). Estimates of throughfall chemistry are consistent with measured data from University of Tennessee. Earlier NO_3^- and SO_4^{2-} throughfall from the IFS are higher than the more recent measured values from University of Tennessee and model simulations during the period of higher SO_2 and NO_x emissions and atmospheric deposition. Measured mineralization of N from the University of Tennessee (1 keq/ha-yr) are less than model simulated rates (2.4 keq/ha-yr). PnET-BGC somewhat underestimated (0.54 vs 0.71 keq/ha-yr) drainage losses of NO_3^- and overestimated Ca^{2+} drainage losses (0.93 vs 0.83 keq/ha-yr) compared to measured fluxes.

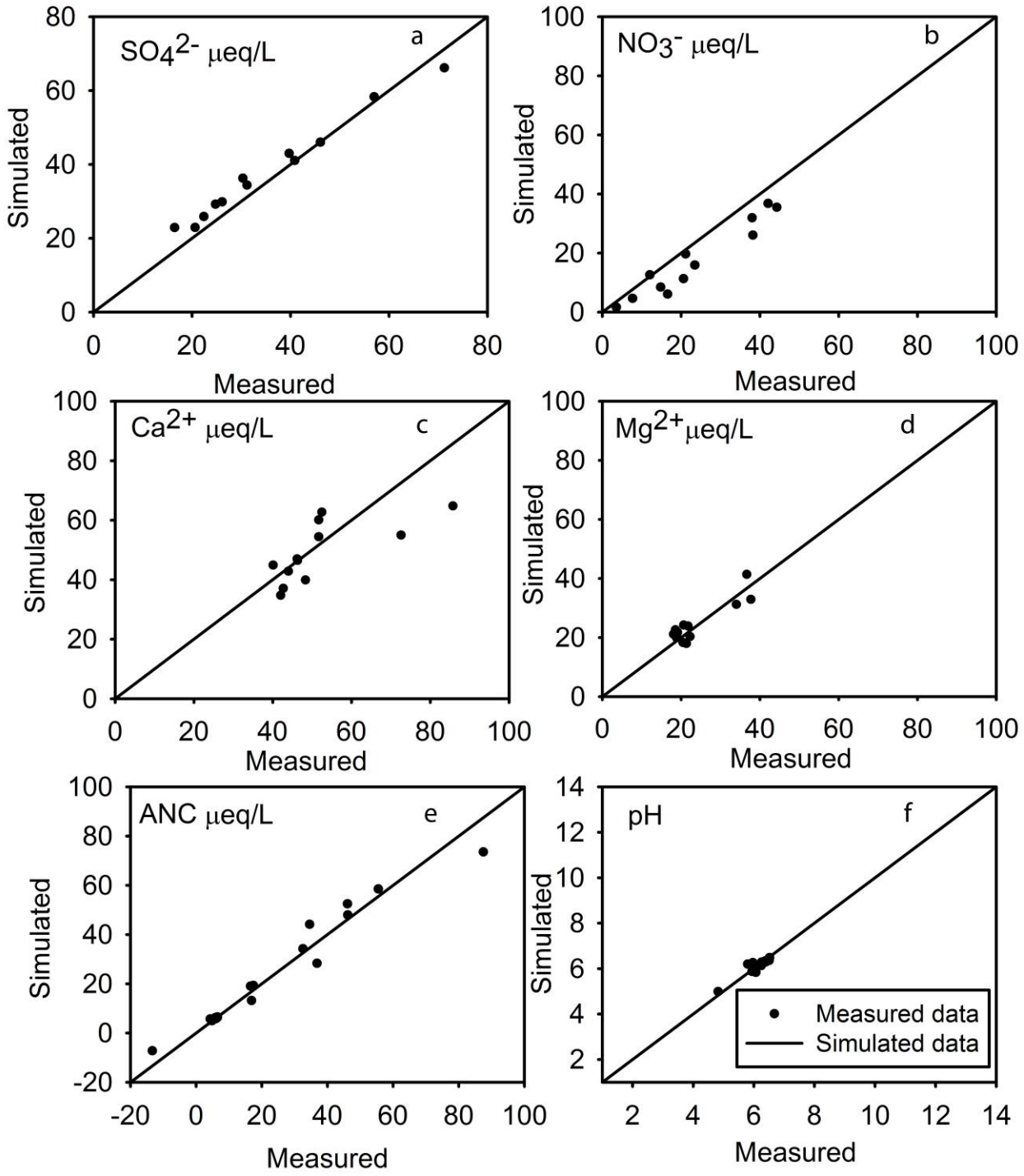

Figure 1. Model comparison between measured and model-predicted mean annual volume-weighted concentrations of selected stream solutes for 12 sites in GRSM. The line is 1:1 line. Observations values are means values for 1994–2008 for each site.

Table 4. Summary of the results of model simulations of mean annual volume-weighted concentrations for selected stream solutes for 12 sites in GRSM. Shown are simulated (S) and observed (O) concentrations and metrics of agreement between measured and model simulated values (NME, NMAE).

	Mg				Ca				NO_3			
	S	*O*	*NME*	*NMAE*	*S*	*O*	*NME*	*NMAE*	*S*	*O*	*NME*	*NMAE*
Noland Divide	24.22	20.67	0.17	0.17	60.11	51.68	0.16	0.17	35.47	44.31	-0.20	0.29
Indian Camp Creek	23.90	21.77	0.10	0.13	64.80	85.76	-0.24	0.23	36.80	42.08	-0.13	0.25
Walker Camp Prong	31.23	34.04	-0.08	0.15	62.72	52.49	0.19	0.22	31.91	38.04	-0.16	0.21
Goshen Prong	18.33	20.49	-0.11	0.26	44.91	40.11	0.12	0.36	19.70	21.17	-0.07	0.29
Lost Bottom Creek	21.13	18.08	0.17	0.12	34.74	42.04	-0.17	0.26	4.65	7.68	-0.39	0.44
Left Prong Anthony	22.61	18.57	0.22	0.24	54.43	51.68	0.05	0.30	15.92	23.48	-0.32	0.31
Pretty Hollow	19.93	18.86	0.06	0.18	37.09	42.68	-0.13	0.33	6.08	16.60	-0.63	0.63
Cosby Creek	41.40	36.69	0.13	0.20	55.00	72.58	-0.24	0.19	26.05	38.24	-0.32	0.33
Sugar Fork	32.91	37.71	-0.13	0.18	39.91	48.34	-0.17	0.22	1.66	3.55	-0.53	0.57
Cannon Creek	17.98	21.34	-0.16	0.22	46.49	46.31	0.00	0.50	11.31	20.60	-0.45	0.45
Thunderhead	21.73	19.10	0.14	0.21	46.98	46.20	0.02	0.30	8.45	14.80	-0.43	0.48
Mill Creek	20.33	22.27	-0.09	0.09	42.85	43.99	-0.03	0.22	12.61	12.07	0.05	0.29

Note: S–model simulation values, O - observed values (most sites between 1995 – 2006; Noland Divide Watershed between 1994-2008); Values represent annual volume weighted concentrations; Units for Mg^{2+}, Ca^{2+}, NO_3^-, SO_4^{2-}, ANC are µeq/L. NME is normalized mean error; NMAE is normalized mean absolute error.

Table 4. (continued)

	SO_4				ANC				pH			
	S	*O*	*NME*	*NMAE*	*S*	*O*	*NME*	*NMAE*	*S*	*O*	*NME*	*NMAE*
Noland Divide	41.05	40.85	0.00	0.10	5.70	4.31	0.32	0.50	6.20	5.80	0.07	0.11
Indian Camp Creek	58.30	56.98	0.02	0.09	13.20	16.88	-0.22	0.43	6.26	5.97	0.05	0.06
Walker Camp Prong	66.16	71.25	-0.07	0.12	-7.23	-13.32	-0.46	0.94	4.99	4.82	0.03	0.04
Goshen Prong	36.26	30.32	0.20	0.22	19.30	17.42	0.11	0.30	5.83	6.07	-0.04	0.05
Lost Bottom Creek	22.90	16.46	0.39	0.38	58.49	55.49	0.05	0.11	6.36	6.50	-0.02	0.03
Left Prong Anthony	29.86	26.12	0.14	0.17	44.15	34.58	0.28	0.26	6.28	6.26	0.00	0.01
Pretty Hollow	22.91	20.62	0.11	0.16	52.45	46.11	0.14	0.16	6.33	6.38	-0.01	0.02
Cosby Creek	46.10	46.08	0.00	0.10	28.30	36.85	-0.23	0.25	6.10	6.27	-0.03	0.04
Sugar Fork	25.88	22.41	0.15	0.17	73.54	87.51	-0.16	0.21	6.48	6.52	-0.01	0.03
Cannon Creek	42.98	39.73	0.08	0.15	19.02	16.59	0.15	0.53	5.87	5.94	-0.01	0.02
Thunderhead	34.39	31.16	0.10	0.12	34.23	32.55	0.05	0.28	6.13	6.25	-0.02	0.04
Mill Creek	29.21	24.78	0.18	0.26	47.92	46.18	0.04	0.10	6.29	6.40	-0.02	0.02

Note: S–model simulation values, O - observed values (most sites between 1995 – 2006; Noland Divide Watershed between 1994 – 2008); Values represent annual volume weighted concentrations; Units for Mg^{2+}, Ca^{2+}, NO_3^-, SO_4^{2-}, ANC are µeq/L. NME is normalized mean error; NMAE is normalized mean absolute error.

Hindcasts (1850–2010) for Stream Chemistry at GRSM

A time series of simulated annual volume weighted concentrations of SO_4^{2-} , NO_3^-, and ANC from 1850–2010 for each of the stream study sites are shown in Figure 2. Pre-industrial stream SO_4^{2-} has a mean of 9.5 $\pm$ 7.1 µeq/L. Three of the study watersheds have some Anakeesta, and those streams have higher pre-industrial SO_4^{2-} than the non-Anakeesta streams (mean SO_4^{2-} for Anakeesta watersheds 13.3 $\pm$ 8.9 µeq/L vs. 8.2 $\pm$ 6.2 µeq/L for non-Anakeesta watersheds). The hindcast simulations generally show increases in stream SO_4^{2-} over the past 150 years with peak values occurring in the 1970s–1980s coinciding with maximum values in SO_2 emissions and SO_4^{2-} deposition in the eastern U.S., decreasing to current values. The mean simulated value for current (1999–2009) SO_4^{2-} is 38.0 $\pm$ 13.5 µeq/L, and this agrees well with the mean measured current value (35.5 $\pm$ 16.1 µeq/L). On average, model simulations suggest that stream SO_4^{2-} in GRSM increased on average 26 $\pm$ 12.5 µeq/L from pre-industrial values (~1850) to present. Although the long-term temporal pattern of increases in stream SO_4^{2-} in response to increases in atmospheric SO_4^{2-} deposition was comparable across the study watersheds, the magnitude of increase in stream SO_4^{2-} was highly variable (Figure 2). The variability in stream SO_4^{2-} response can partially be explained by variability in atmospheric SO_4^{2-} deposition superimposed on variation in elevation ([stream SO_4^{2-} concentration (µeq/L)]=0.019[elevation (m)]+17.2; r^2=0.15) and variation in soil SO_4^{2-} adsorption capacity ([Stream SO_4^{2-} concentration (µeq/L)]= -0.25[SO_4^{2-} adsorption capacity (meq/kg)]+46.8; r^2=0.23).

Simulations of pre-industrial stream NO_3^- estimated concentrations are low for the study watersheds (1.2 $\pm$ 0.7 µeq/L; Figure 2). Model hindcasts showed low stream NO_3^- until the 1950s and 1960s when some study watersheds started to show increasing leaching losses which have continued to present. Average current simulated annual volume-weighted stream NO_3^- (17.6 $\pm$ 12.4 µeq/L) compares well with current measured values (23.2 $\pm$ 13.3 µeq/L). The mean increase in stream NO_3^- from pre-industrial values to present is 22 $\pm$ 12.2 µeq/L, with a large range from 39.5 $\pm$ 4.5 µeq/L at Indian Camp Creek Watershed – 3.2 $\pm$ 3.7 µeq/L at Sugar Fork. This variation in simulated stream NO_3^- in part coincides with variation in watershed elevation ([NO_3^- concentration (µeq/L)] = 0.028[elevation (m)] -3.59; r^2=0.40).

There is considerable variability in watershed sensitivity to acidic deposition among the study sites. Projections of pre-industrial ANC (ANC projected for 1850) at these sites ranged from 28 µeq/L at Noland Divide – 107 µeq/L at Sugar Fork, with a mean of 70.8 $\pm$ 10.5 µeq/L. Variations in preindustrial stream ANC at GRSM were somewhat related to watershed elevation ([ANC (µeq/L)] = -0.029[elevation (m)] + 61.9; r^2=0.15). Hindcasts of stream ANC from 1850 – present coincide with increases in acidic deposition and leaching of SO_4^{2-} and NO_3^-. Simulated current mean annual volume-weighted ANC is 32.8 $\pm$ 21.5 µeq/L which is consistent with the current measured mean ANC (33.1 $\pm$ 25.9 µeq/L). Hindcasts suggest that on average across the 12 GRSM modeled streams, acidic deposition resulted in a decrease in ANC of 37.6 µeq/L from pre-industrial values – present. Model simulations indicate that current values of stream ANC are correlated with estimates of pre-industrial ANC values (r^2 = 0.38; Figure 3).

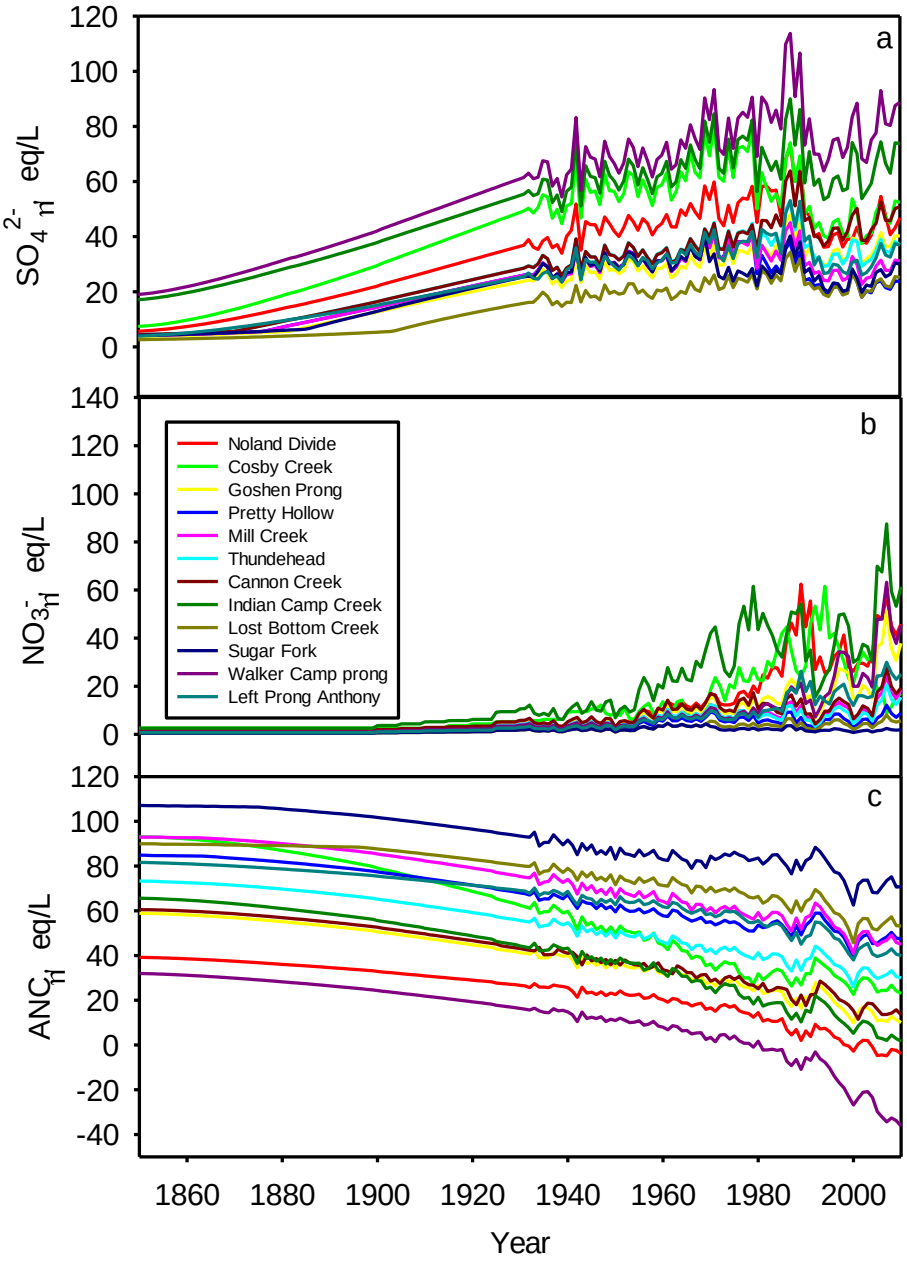

Figure 2. Simulations of hindcasts of SO_4^{2-}, NO_3^-, and acid neutralizing capacity (ANC) for stream chemistry sites in GRSM.

Future Projections

For each of the study watersheds, future projections of hypothetical decreases in NO_3^- and SO_4^{2-} deposition individually and together since 2008 were made. To illustrate this response, this study shows detailed hindcasts and the suite of forecast projections for one of GRSM watersheds, Goshen Prong, indicating the response to projected decreases in NO_3^- deposition with: (a) SO_4^{2-} deposition remaining at current values; (b) decreases in SO_4^{2-} deposition with NO_3^- deposition remaining at current elevated values; and (c) decreases in both NO_3^- and SO_4^{2-} deposition (Figure 3). Simulations of hindcast and future forecast projections for all 12 study watersheds are given in Appendix 1.

Goshen Prong (~1046m) exhibits relatively high NO_3^- leaching (~21 µeq/L), is sensitive to acidic deposition (ANC=21 µeq/L) and is a 303d listed stream. Current model simulations of stream chemistry at Goshen Prong generally agreed with measured values (i.e., SO_4^{2-} NME = 0.20; NO_3^- NME = -0.07; Ca^{2+} NME = 0.12; ANC NME = 0.11; pH NME = -0.04). The hindcast projections show a pattern of long-term increases in stream NO_3^- which depicts in the model the watershed approaching a condition of N saturation. Simulations of a range of future conditions of NO_3^- deposition suggest that the watershed would be responsive to changes in NO_3^- loading (Figure 3a). In the absence of controls on NO_3^- deposition, the watershed is projected to exhibit increases in leaching losses of NO_3^- to high concentrations (~100 µeq/L) through about 2200 resulting in marked decreases in ANC and pH. Incremental future reductions on NO_3^- deposition lessen the extent and rate of increases in NO_3^- leaching and mitigate decreases in pH and ANC. These changes in NO_3^- leaching alter the biogeochemical dynamics of the soil exchange complex in the decades following changes in deposition. PnET-BGC has a pH-dependent algorithm for soil SO_4^{2-} adsorption (Gbondo-Tugbawa et al., 2001). Increases in leaching of NO_3^- under the elevated NO_3^- deposition scenarios protonates soil surfaces, increasing soil adsorption of SO_4^{2-} subtly decreasing stream SO_4^{2-}. Increases in NO_3^- leaching also enhances the displacement of Ca^{2+} (and other base cations) from soil cation exchange sites increasing Ca^{2+} leaching in stream water for a period until the available soil pool becomes depleted.

The suite of SO_4^{2-} deposition reduction scenarios (with no decreases in NO_3^- deposition) show that decreases in SO_4^{2-} in Goshen Prong and other watersheds in GRSM will effectively lower SO_4^{2-} concentrations in stream water (Figure 3b). However, as NO_3^- deposition is unchanged, ongoing elevated NO_3^- drives the watershed toward a condition of N saturation and increasing concentrations of NO_3^- in stream water. As a mobile anion, NO_3^- strongly contributes to the continued acidification of Goshen Prong, resulting in continuing decreases in ANC and pH. Simultaneous control of NO_3^- and SO_4^{2-} is the most effective approach to decrease concentrations of total strong acid anion concentrations in stream water of GRSM watersheds arresting acidification and allowing for limited recovery. Note that even under marked decreases in NO_3^- deposition as the forest biomass matures, NO_3^- leaching losses are expected to increase over time, because GRSM is an unmanaged forest.

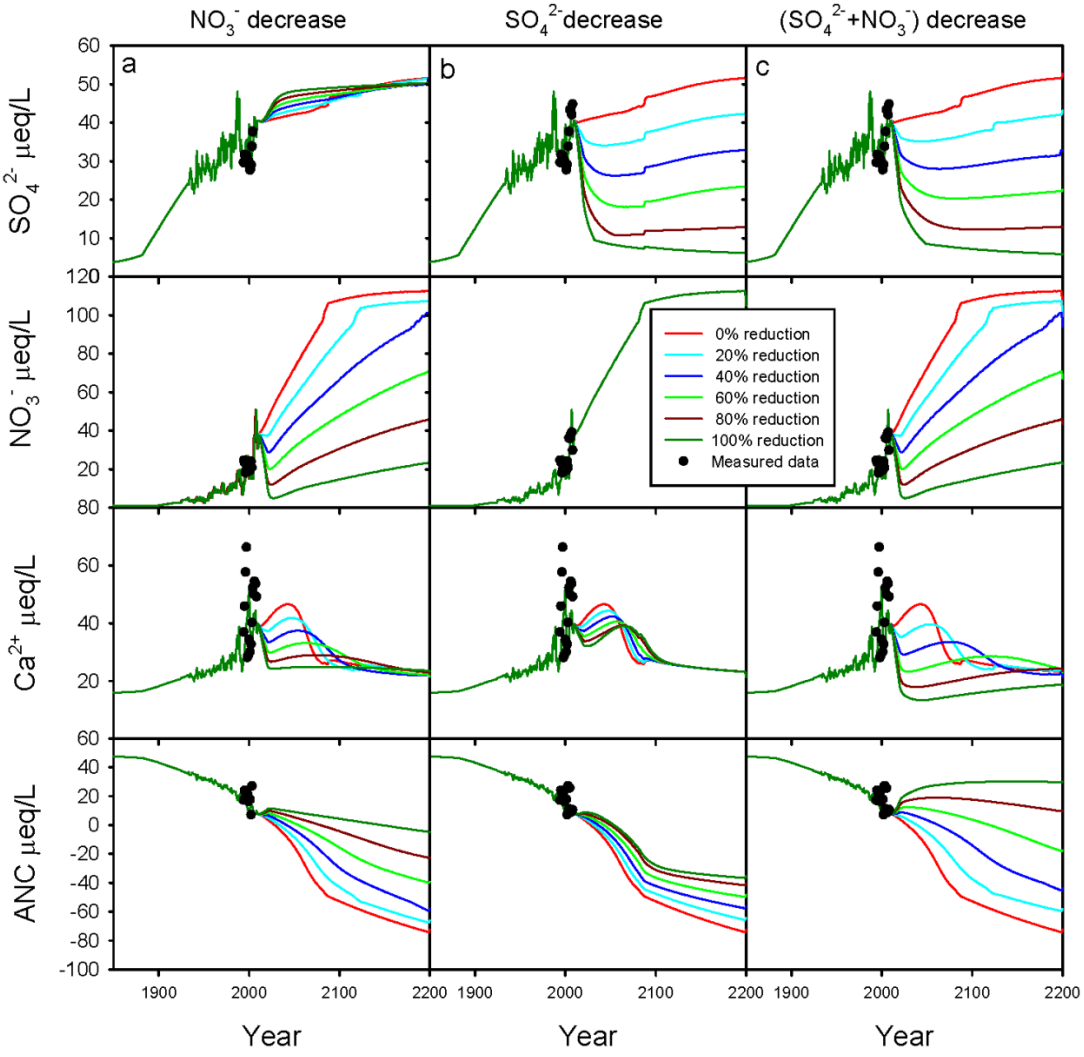

Figure 3. Time series of stream SO_4^{2-}, NO_3^-, Ca^{2+}, ANC and pH for Goshen Prong watershed (y-axis) that include hindcasts and future projections to atmospheric deposition decreases in: (a) NO_3^- only, (b) SO_4^{2-} only, and (c) both NO_3^- and SO_4^{2-}. Also shown are measured values.

Factors Affecting Historical Acidification and Recovery

Historical acidification (HA) is defined as the change in simulated ANC from the pre-industrial value of 1850 to the current value (2010). We evaluated characteristics of the 12 GRSM study watersheds to assess factors that control HA. Modeled HA for GRSM watersheds increased with decreasing pre-industrial estimates of ANC ranging from 54.2 µeq/L at acid sensitive Walker Camp Creek – 19.6 µeq/L at less sensitive Sugar Fork (Figure 4a). The lower the pre-industrial estimated ANC, the greater the modeled change (HA) in comparison to current ANC values. For example, the HA of acid sensitive Walker Camp Prong is 54.2 µeq/L (pre-industrial ANC: 41.0 µeq/L; current ANC: -13.2 µeq/L) compared with the less sensitive Sugar Fork site of 19.6 µeq/L (pre-industrial ANC: 107.1 µeq/L; current ANC: 87.5 µeq/L). We observed a negative relation between HA and estimated preindustrial ANC (1850) (r^2=0.33), suggesting the lower the preindustrial ANC the greater the extent of acidification from acid deposition (Figure 4a). We found a positive relation between current SO_4^{2-} + NO_3^- deposition and HA (r^2=0.66; Figure 4b), indicating the greater the input of acidic deposition the greater the historical acidification. The extent of HA also decreases with increases in estimated soil SO_4^{2-} adsorption capacity (r^2= 0.19; Figure 4c). We conducted multiple regression analysis of HA with total current SO_4^{2-} + NO_3^- deposition, historical ANC and soil SO_4^{2-} adsorption capacity which explained most of the watershed variation in the extent of HA.

HA (µeq/L) =35.9+ 7.4×[current SO_4^{2-} + NO_3^- deposition (keq/ha-yr)] + 0.002×[preindustrial ANC (µeq/L)] -0.06×[SO_4^{2-} adsorption capacity (meq/kg)] (r^2=0.73)

We define maximum recovery (MR) as the difference between stream ANC projected for 2200 under the scenario which atmospheric NO_3^- + SO_4^{2-} deposition are lowered to pre-industrial values and the scenario which atmospheric NO_3^- + SO_4^{2-} deposition remains at current deposition. As observed for HA, MR decreases with increasing current (2010) ANC (r^2= 0.65; Figure 4d; 21.8 µq/L – 121.0 µeq/L). We found a similar relationship between MR and preindustrial (historical) ANC (r^2 = 0.62; Figure 4e). In contrast, MR was positively related to current NO_3^- + SO_4^{2-} deposition (r^2=0.37; Figure 4f).

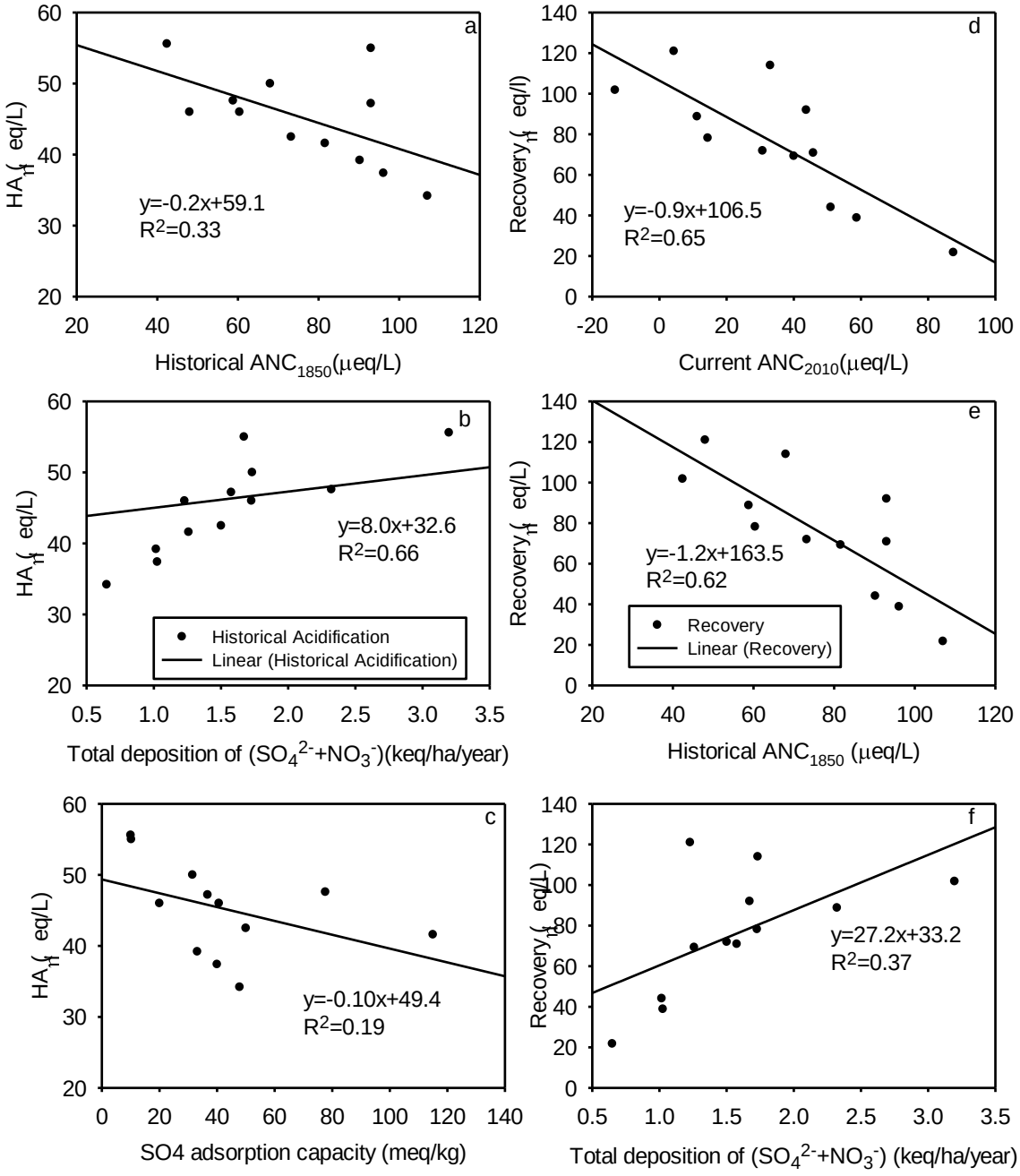

Figure 4. Relationships between (a) preindustrial ANC(1850); (b) current total deposition of SO42- +NO3- ; and (c) estimated soil sulfate adsorption capacity with historical acidification HA; ANC in 1850 – ANC in 2010). Relationships between (d) current ANC (2010); (e) preindustrial ANC(1850) ; and (f) current total deposition of SO_4^{2-} +NO_3^- with maximum recovery (MR) ANC under decreases in total deposition of SO_4^{2-} +NO_3^- to preindustrial values in 2200). Results of linear regression analysis are shown.

Projections of DCLs

We are ultimately interested in developing CLs and DCLs for all streams in the entire GRSM. To illustrate how this extrapolation might be accomplished using simulations from the 12 study watersheds, we interpolated the results of stream ANC projections for a hypothetical year (2050) from future decreases in NO_3^- + SO_4^{2-} deposition to a series of target ANC values: 0, 20 and 50 µeq/L. These target ANC values were selected because they are values that have been selected as potential target ANC in the U.S. CL assessment (USEPA, 2009). We found that the DCL in 2050 necessary to achieve a given ANC target for GRSM sites was approximately a linear function of current stream ANC. DCLs of NO_3^- + SO_4^{2-} deposition for the 12 study stream ranged from 0–12 keq/ha-yr to reach an ANC of 0 µeq/L by 2050; 0–9 keq/ha-yr to reach ANC of 20 µeq/L by 2050; and 0–4.5 keq/ha-yr to reach an ANC µeq/L of 50 by 2050. Note that for some study streams, ANC targets cannot be met under the deposition reductions and time periods used for this study (Table 9). From PnET-BGC projections we developed three empirical relationships of NO_3^- + SO_4^{2-} deposition necessary to achieve a target DCL (Figure 5). These projections suggest that the higher the target ANC the lower the DCL necessary to achieve this value of ANC. Moreover, the lower the current stream ANC the lower the DCL necessary to achieve a target ANC value by 2050. As most stream sites modeled have ANC values <50 µeq/L, the modeled relationships suggest that this target ANC will not be achievable at many low ANC sites.

In addition, we conducted simulations for three impaired streams (Goshen Prong, Cannon Creek, Noland Divide) to determine the level of deposition necessary to recovery the ANC to alleviate the impaired condition based on criteria established by the State of Tennessee Department of Environmental Conservation (TDEC). The TDEC developed TMDLs for acid impaired streams by empirically estimating the ANC value that would correspond to a pH of 6.0 based on a linear regression analysis from measured paired observations. For Goshen Prong the target ANC is around 18 µeq/L, while the target ANC for Cannon Creek is about 19 µeq/L. TDEC did not determine a target ANC for Noland Divide, but using National Park Service and University of Tennessee data we used the TDEC approach to estimate a target ANC of 22 µeq/L for Noland Divide. We used the suite of simulations of different levels of decreases in SO_4^{2-} and NO_3^- deposition for these impaired sites to determine the level of deposition necessary to achieve the target ANC values.

Our analysis suggests that decreasing SO_4^{2-} + NO_3^- deposition to 0.9 keq/ha-yr by 2020 (48% decrease from current values) would allow the target ANC to be achieved by 2050 for Cannon Creek. We did not examine combinations of changes in SO_4^{2-} and NO_3^- deposition that would allow the target to be reached. Nor did we evaluate lower levels of deposition that could achieve this target over a shorter period. This could be done in the future. Simulations suggest that the target ANCs could not be achieved for Noland Divide or Goshen Prong by 2050.

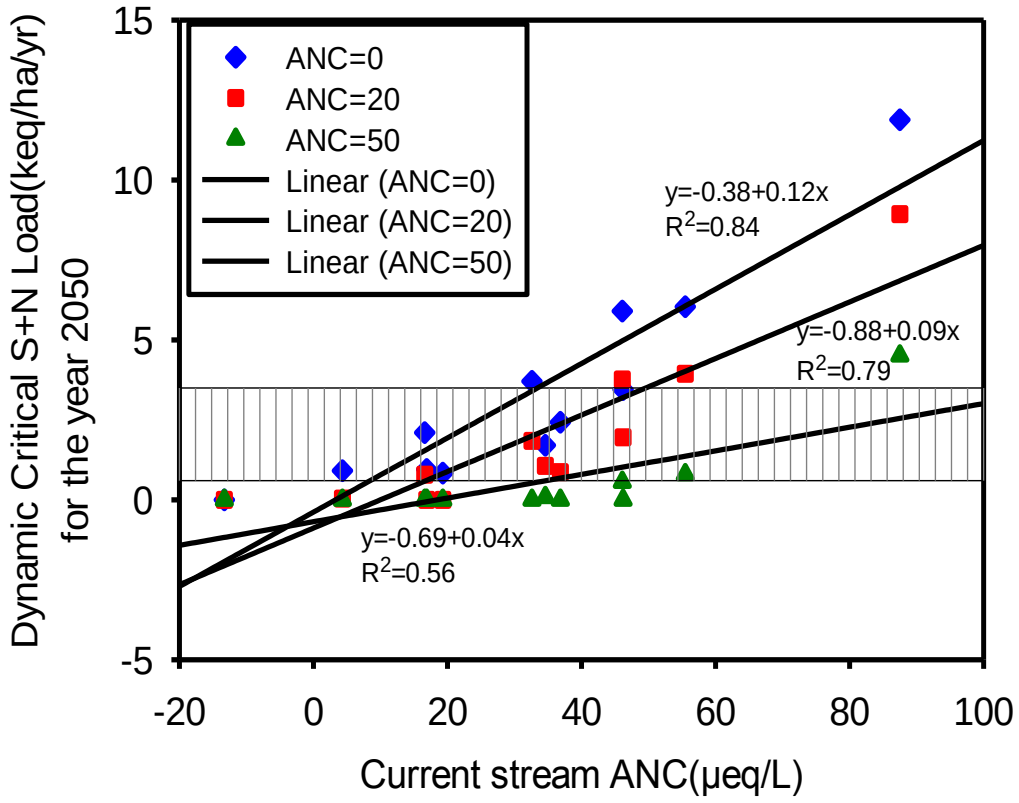

Figure 5. Empirical relationships between current ANC of GRSM streams and the deposition of NO3- + SO42- necessary to achieve target ANC values of 0, 20 and 50 µeq/L in 2050. These values were developed from simulations from 12 study sites with PnET-BGC. Also shown as cross hatching the range of NO_3^- + SO_4^{2-} deposition currently observed in GRSM.

4. Discussion

Model Performance

Model simulations of stream chemistry in GRSM generally matched observed values. SO_4^{2-} simulations compared well with observations at most sites (NME <0.20; Figure 1a), except Lost Bottom Creek (NME = 0.39), whose watershed has among the highest soil SO_4^{2-} adsorption capacity and lowest stream SO_4^{2-} concentration (16.5 µeq/L) among the study watersheds (Grell, 2010). Generally, simulations of SO_4^{2-} showed that all sites were slightly overpredicted compared with observed values, except for Walker Camp Prong (NME = -0.07). Walker Camp Prong is a high elevation site (1,168 m) and has the highest SO_4^{2-}concentration (71.3 µeq/L) among the study sites. Previous studies have shown that total SO_4^{2-} deposition generally increases with increasing elevation (Shubzda et al., 1995; Lovett et al., 1997; Weathers et al., 2006). Although the elevation of Noland Divide Watershed (1,798m) is higher than Walker Camp Prong, stream SO_4^{2-} concentrations are lower. Soils at Walker Camp Prong are characterized by high SO_4^{2-} concentrations in the B/C horizon compared with other GRSM sites (Grell, 2010). Anakeesta, which contains pyrite, is abundant in Walker Camp Prong (Table 1). The exposure of soil caused by a natural slide in the headwaters of Walker Camp Prong likely enhances mineral oxidation to produce SO_4^{2-}, resulting in elevated stream concentrations (Flum and Nodvin, 1995). Currently S oxidation and release is not explicitly depicted in PnET-BGC. We estimate historical rates of S weathering for each watershed based on reconstructions of changes in atmospheric S deposition and soil SO_4^{2-} adsorption. Qualitatively, watersheds with Anakeesta coupled with land disturbance have higher stream SO_4^{2-} than those without Anakeesta, and thus we depict this through increases in S weathering rates in the model. We assumed that rates of watershed S weathering remained constant through simulations. However, if S weathering rates are changing particularly for watersheds with an abundance of Anakeesta, this would represent a variable and potentially important input of S that was not depicted in the model and would challenge the accuracy of model hindcasts and projections.

One of the most important but poorly constrained aspects of simulations of the dynamics of S in GRSM watersheds is soil SO_4^{2-} adsorption, and the varying ability of SO_4^{2-} to bind to the soil surfaces associated with changes in soil pH. Process studies and watershed mass balances have demonstrated that a large fraction of SO_4^{2-} entering the watershed from atmospheric deposition, historically and currently, is retained by SO_4^{2-} adsorption (Johnson and Lindberg, 1992; Cai et al., 2012). Estimates of soil SO_4^{2-} adsorption are obtained through previous soil adsorption isotherms (Church et al., 1989) and model calibration. PnET-BGC depicts soil SO_4^{2-} adsorption as a pH-dependent process, which increases with soil acidification and decreases in pH and decreases with increases in soil pH. This algorithm has been well-tested in glaciated landscapes (Gbondo-Tugbawa and Driscoll, 2002), but not for unglaciated soils such as GRSM. Additional experimentation and improved parameterization should be conducted to improve characterization of SO_4^{2-} adsorption and its pH-dependence in GRSM soils.

PnET-BGC generally underestimated stream NO_3^- across the study sites (Figure 1b). Land disturbance strongly affects NO_3^- losses in forest ecosystems (Goodale and Aber, 2001; Aber et al., 2003). Historical land disturbance for GRSM was estimated from National Park Service records

(Pyle, 1985). However, these historical records are incomplete. For instance, forest disturbance associated with climatic events have only been quantified to a limited extent for GRSM. In addition, historical land disturbance data for model inputs were estimated by digitizing area of land disturbance. The amount of dead and lost biomass from historical land disturbance is highly uncertain for individual watersheds. Moreover, atmospheric deposition is an important and heterogeneous component of inputs of N (and other elements) in the mountainous terrain of GRSM (Weathers et al., 2006), and simplification of current and past atmospheric deposition estimates undoubtedly contributes to errors in model simulations.

Simulated stream Ca^{2+} generally was in good agreement with observed values (NME <0.19; Figure 1c). The Ca^{2+} weathering rate is not measured directly. Rather, cation weathering is determined by model calibration and assumed to be constant through the simulation period. Gbondo-Tugbawa et al. (2001) showed that overprediction or underprediction of strong acid anions (i.e., SO_4^{2-}, NO_3^-) by PnET-BGC affect simulated losses of Ca^{2+} from exchange sites in soil because strong acid anions facilitate leaching basic cations.

Model simulations of current stream ANC were in good agreement with measured values for most sites (NME < 0.15; Figure 1e). The major exception was Walker Camp Prong, which exhibited a NME of -0.46 in model simulation of ANC. Overprediction of basic cations (NME=0.19) coupled with underprediction of strong acid anions (SO_4^{2-} NME: -0.07, NO_3^- NME: -0.16) led to a discrepancy in ANC for Walker Camp Prong.

Mass balances for Noland Divide Watershed and Goshen Prong Watershed

Noland Divide Watershed is a high elevation, acid-sensitive watershed. It has been investigated since the Integrated Forest Study in late 1980s (Johnson and Lindberg, 1992). Researchers from the University of Tennessee have collected biweekly samples of wet deposition, throughfall, soil leachate and stream water samples since 1991 (Cai et al., 2010). Element mass balances were performed for Noland Divide Watershed based on model simulations, which were compared with measured data to provide a test of the model. Goshen Prong Watershed is an acid sensitive watershed and also one of 12 acid-impaired sites at GRSM. In order to evaluate ANC generation and losses though ecosystem changes, an ANC budget was done to compare ANC in pre- industrial time, current conditions (2010) and in the future.

Mass Balance for Noland Divide Watershed

Model simulations for Noland Divide Watershed for the current period (1994–2008) suggest that NO_3^- has been primarily produced from mineralization of soil organic N and nitrification (1.7 keq/ha-yr) (Table 5) and secondarily from atmospheric N deposition (1.0 keq/ha-yr) based on model simulation. The supply of NO_3^- from internal sources (i.e., mineralization, nitrification) represents an indirect form of atmospheric N deposition that has been cycled through the ecosystem. Simulated throughfall NO_3^- deposition (1.0 keq/ha-yr) (Table 5) was close to measured values from 1999–2006 (0.9 keq/ha-yr) while lower than earlier measurements from the IFS (1.4 keq/ha-yr) due to recent declines NO_3^- deposition (Cai et al., 2012). There was little difference between measured and simulated throughfall NH_4^+ (simulated 0.3 keq/ha-yr; 1991–2006 average 0.3 keq/ha-yr). Simulated plant uptake of NH_4+ (0.9 keq/ha-yr) was much larger than estimates from the IFS (0.3 keq/ha-yr).

Of the total 2.7 keq/ha-yr NO_3^- input to Noland Divide Watershed, most (2.3 keq/ha-yr) was retained through net plant uptake and soil retention (Table 5). Stream export of NO_3^- from Noland Divide Watershed is simulated to be 0.54 keq/ha-yr (Table 6); around 40% of annual atmospheric NO_3^- deposition was discharged by stream water. However model simulations suggest large rates of N accumulation within the watershed and large internal N cycling.

Simulations suggest that SO_4^{2-} inputs to Noland Divide Watershed primarily occur from throughfall (1.8 keq/ha-yr; wet, dry and cloud deposition) and net mineralization of soil organic S (0.8 keq/ha-yr). Simulated losses include net plant S uptake (0.8 keq/ha-yr), net soil SO_4^{2-} sorption (1.2 keq/ha-yr) and exported by drainage losses (0.6 keq/ha-yr). As atmospheric S deposition exceed stream SO_4^{2-} losses, model simulations indicate that SO_4^{2-} inputs are largely retained by soil SO_4^{2-} adsorption. Potentially this process will delay ecosystem recovery from acidification if soil SO_4^{2-} that has accumulated under historical conditions of elevated atmospheric SO_4^{2-} deposition desorbs under future conditions of decreases in atmospheric SO_4^{2-} deposition (Driscoll et al., 2001).

Calcium inputs to Noland Divide Watershed were simulated to be mainly supplied from soil mineralization (1.7 keq/ha-yr), throughfall (0.9 keq/ha-yr), desorption from the soil exchange complex (0.63 keq/ha-yr) and weathering (0.27 keq/ha-yr) (Table 5). Calcium inputs were consumed by plant uptake (2.4 keq/ha-yr) and stream losses (0.9 keq/ha-yr). The model estimated throughfall Ca^{2+} (0.9 keq/ha-yr) was similar to measured values from IFS and the University of Tennessee (0.9 keq/ha-yr). However, simulated watershed export of Ca^{2+} (0.9 keq/ha-yr) was greater than measured values (1991–2006; 0.8 keq/ha-yr).

Table 5. Available measurements and model simulations of element fluxes for Noland Divide Watershed. UT measured values are mean annual values for 1994–2008. IFS measurements were made during 1986–1989.

Site	NH4+ (keq/ha-yr)			NO3- (keq/ha-yr)			SO42- (keq/ha-yr)			Ca2+ (keq/ha-yr)		
	IFS	UT	*M	IFS	UT	*M	IFS	UT	*M	IFS	UT	*M
Through fall Deposition	0.02	0.3	0.29	1.40	0.9	1.02	2.5	2	1.82	0.94	0.9	0.88
Weathering Rate			0	0		0			0.075	0.27		0.27
Mineralization		1.0	2.38			0			0.82			1.7
Nitrification			-1.69			1.69			0			0
Plant uptake			-0.91	-1.89		-2.27	-0.22		-0.84	-0.43		-2.44
Sorption						0			-1.24			0.63
Drainage losses		-0.02	0		-0.71	-0.54		-0.64	-0.64		-0.83	-0.93
Total input			2.67			2.71			2.71			3.48
Total output			2.60			2.81			2.73			3.37

Note: Measured data for throughfall, weathering rate, mineralization, nitrification, plant uptake, sorption, drainage losses are from University of Tennessee (UT) and the Integrated Forest Study (IFS). Simulation values are average from 1994–2008. Positive values indicate ecosystem inputs. Negative values indicate ecosystem losses.

*M denotes model

Element and ANC Budgets for Goshen Prong Watershed (GPW)

From model simulations, we conducted element and ANC budgets for Goshen Prong Watershed for historical (1850–1860), current (1999–2009) (Table 6) and potential future conditions (Table 7). We compared element and ANC budgets from model calculations for two future scenarios: constant deposition (0% decrease) and 20% incremental decreases in deposition to preindustrial conditions (100% reduction of combined SO_4^{2-} and NO_3^- deposition) in 2200. The mass balance calculations considered inputs of atmospheric deposition, internal reactions including soil weathering, vegetation uptake, soil sorption, mineralization, nitrification, and the output of drainage losses.

During the preindustrial period (1850–1860), model simulations suggest that S and NH_4^+ are mainly supplied to the watershed by mineralization and atmospheric deposition is relatively low (Table 6). Historical mineralization inputs of S (0.5 keq/ha-yr) and NH_4^+ (4.3 keq/ha-yr) are balanced by equivalent rates of vegetation uptake. Currently, rates of soil S mineralization are approximately balanced by plant uptake, although rates of internal S cycling (weathering processes, S uptake, soil sorption, mineralization, nitrification and drainage losses) have approximately doubled under the current increases in atmospheric S deposition (1.2 keq/ha-yr. Inputs of atmospheric N deposition

have altered the cycling of N within the ecosystem, by increasing rates of N mineralization to NH_4 (5.7 keq/ha-yr) during current conditions. A relatively large fraction of mineralized N is nitrified to NO_3 (2.8 keq/ha-yr; 49%). As a result, a fraction of vegetation N uptake occurs as NO_3^- (49%) in contrast to the overwhelmingly vegetation uptake of NH_4^+ under preindustrial conditions (~100%). Model simulations also suggest that under current atmospheric deposition there has been an uncoupling of base cation cycling (Table 6) in Goshen Prong Watershed. Under preindustrial conditions, vegetation uptake of base cations (i.e., Ca, Mg, K) was balanced by the supply from mineralization. Following historical acidification, base cation cycling has been enhanced but vegetation uptake (4.2 keq/ha-yr) exceeds supply from mineralization (3.6 keq/ha-yr). The simulations suggest that additional cations to support vegetation growth and accelerated stream losses (1.3 keq/ha-yr) are largely supplied by leaching from the soil exchange complex (0.76 keq/ha-yr) resulting in soil base cation depletion.

ANC budgets showed that mineralization and weathering are important processes generating ANC today and under pre-anthropogenic conditions. However, currently the ANC budget has shifted markedly due to increases in atmospheric deposition of SO_4^{2-} and NO_3^-, increases in nitrification, increases in NO_3^- uptake by vegetation (4.2 keq/ha-yr), and increases in the release of base cations from soil exchange sites (0.76 keq/ha-yr). Nitrification plays an important role in the decrease in the current watershed ANC budget because NH_4^+ is readily nitrified into NO_3^-, decreasing ANC.

In 2200, Goshen Prong Watershed shows contrasting patterns of N cycling under the two different future deposition scenarios (Table 7). Under the no change in atmospheric deposition scenario, simulations indicate that the watershed N cycling continues to increase as the watershed progresses toward a condition of N saturation. The cycling of N increasingly occurs through NO_3^-, as elevated rates of nitrification supply much of the N retained by vegetation (70%). Drainage losses of NO_3^- are projected to be very high (1.3 keq/ha-yr). ANC budgets for 2200 show that under the no change in acid deposition scenario, very high rates of acidity (0.8 keq/ha-yr) are lost from the watershed due to high simulated rates in N mineralization and nitrification. In contrast under the 100% decrease in atmospheric deposition scenario (return to preindustrial conditions) in 2200, Goshen Prong Watershed improves ANC (0.40 keq/ha-yr) due to decreases in atmospheric S and N deposition and associated decreases in N mineralization and nitrification (Table 7). Note that forest maturation and lack of disturbance contributes to the acceleration of a condition of N saturation in GRSM watersheds.

Table 6. Element and ANC budgets for Goshen Prong Watershed for preindustrial (1850–1860) and current (1999–2009) periods. Preindustrial data (1850–1860) is from Shannon's ASTRAP model. Current period (1999–2009) is from model parameterization or simulation.

Flux	C_B (keq/ha-yr)		NO_3^- (keq/ha-yr)		SO_4^{2-} (keq/ha-yr)		NH_4 (keq/ha-yr)		ANC (keq/ha-yr)	
Period	1850–1860	1999–2009	1850–1860	1999–2009	1850–1860	1999–2009	1850–1860	1999–2009	1850–1860	1999–2009
Deposition	0.0	0.1	0.2	1.7	0.1	0.5	0.0	0.3	-0.2	-2.1
Weathering rate	0.7	0.7	0.0	0.0	0.0	0.0	0.0	0.0	0.7	0.7
Canopy exchange	0.0	0.4	0.0	0.0	0.0	0.0	0.0	-0.1	0.0	0.4
Uptake	-2.8	-4.2	-0.1	-4.2	-0.5	-1.2	-4.4	-3.1	-6.5	-1.9
Soil sorption	0.0	0.8	0.0	0.0	0.0	0.0	0.0	0.0	0.0	0.7
Mineralization	2.7	3.6	0.0	0.0	0.5	1.2	4.3	5.7	6.5	8.1
Nitrification	0.0	0.0	0.0	2.8	0.0	0.0	0.0	-2.8	0.0	-5.6
Drainage losses	-0.6	-1.3	0.0	-0.4	-0.1	-0.5	0.0	0.0	-0.6	-0.2
Sources	3.4	5.5	0.2	4.5	0.6	1.7	4.4	6.0	7.2	9.9
Sinks	-3.4	-5.5	-0.1	-4.6	-0.6	1.7	-4.4	-6.0	-7.3	-9.8

Note: Measured data for throughfall, weathering rate, mineralization, nitrification, plant uptake, sorption, drainage losses are from University of Tennessee (UT) and the Integrated Forest Study (IFS). Simulation values are average from 1994–2008. Positive values indicate ecosystem inputs. Negative values indicate ecosystem losses.

Table 7. Element and ANC budgets for hypothetical recovery of Goshen Prong Watershed. Element fluxes values are shown for 2200 comparing values under scenarios of current deposition (without reduction) with 100% decrease in anthropogenic deposition to preindustrial values.

Flux	C_B (keq/ha-yr)		NO_3^- (keq/ha-yr)		SO_4^{2-} (keq/ha-yr)		NH_4^+ (keq/ha-yr)		ANC (keq/ha-yr)	
Period	Without	100%	Without	100%	Without	100%	Without	100%	Without	100%
	Reduction	Reduction	Reduction	Reduction	Reduction	Reduction	Reduction	Reduction	Reduction	Reduction
Deposition	0.1	0.1	1.7	0.2	0.5	0.1	0.3	0.3	-1.9	0.2
Weathering rate	0.7	0.7	0.0	0.0	0.0	0.0	0.0	0.0	0.7	0.7
Canopy exchange	0.3	0.0	0.0	0.0	0.0	0.0	0.0	0.0	0.3	0.0
Uptake	-3.7	-3.3	-17.0	-4.2	-1.6	-0.6	7.5	-3.0	22.4	-1.6
Soil sorption	0.0	0.1	0.0	0.0	0.0	0.0	0.0	0.0	0.3	0.0
Mineralization	3.4	3.2	0.0	0.0	1.6	0.6	8.9	7.2	10.7	9.9
Nitrification	0.0	0.0	16.6	4.3	0.0	0.0	-16.6	-4.3	-33.1	-8.7
Drainage losses	-0.8	-0.8	-1.3	-0.3	-0.6	-0.1	0.0	0.0	0.8	-0.4
Sources	4.5	4.1	18.3	4.5	2.1	0.7	16.6	7.4	35.0	10.7
Sinks	-4.5	-4.1	-18.3	-4.5	-2.1	-0.6	-16.6	-7.4	-35.0	-10.7

Comparison of controls on SO_4^{2-}, NO_3^- and NH_4^+deposition

In order to evaluate ecosystem responses to relative controls on SO_4^{2-} and NO_3^- deposition, we ran the model under future projections of hypothetical decreases in SO_4^{2-}, NO_3^- and NH_4^+ deposition individually, and in combination. Model projections suggest that under no additional controls of SO_4^{2-} (or NO_3^-) deposition (0% reduction, constant deposition), the ANC of Goshen Prong is projected to continue to acidify, decreasing to -73 µeq/L by 2200 (Figure 4b (or 3a). If atmospheric SO_4^{2-} deposition is eliminated (100% reduction to preindustrial conditions) with no change in atmospheric NO_3^-deposition, ANC was projected to decrease to -36 µeq/L by 2200. Sulfate adsorption plays an important role in regulating the acid-base status of streamwater particularly in the decades immediately following decreases in atmospheric SO_4^{2-} deposition. Soil SO_4^{2-} adsorption is depicted in PnET-BGC to be a pH-dependent process in which adsorbed OH^- ligand is replaced by SO_4^{2-} to decrease the solution SO_4^{2-} concentration and consequently increase ANC. The relationship between HA (historical acidification) and SO_4^{2-} adsorption capacity among the different watershed sites showed that HA was limited by soil SO_4^{2-} adsorption capacity. In PnET-BGC soil SO_4^{2-} adsorption is assumed to be reversible. As a result, legacy SO_4^{2-} that has accumulated in soil under historical elevated acidic deposition can completely desorb under decreases in atmospheric SO_4^{2-} deposition and serve to delay stream recovery.

When atmospheric deposition of NO_3^- was decreased by 100% to preindustrial conditions, the projected ANC responses in Goshen Prong Watershed were similar to SO_4^{2-} responses (Figure 4a). When atmospheric NO_3^- deposition is decreased to the same level as historical deposition (100% decrease scenarios) with no change in atmospheric SO_4^{2-} deposition, ANC is projected to be increased from -73 (highly acidic) to 0 µeq/L by 2200. In GRSM, ANC = 0 is a lethal threshold for brook trout (*Salvelinus fontinalis)* and rainbow trout (*Oncorhynchus mykiss;* Cai and Schwartz, 2012). These conditions indicate that decreases in NO_3^- deposition will be important in decreasing water acidity and improving habitat for the aquatic community. These simulations show that under this maximum range of conditions, stream NO_3^- concentration in Goshen Prong decrease from 113 µeq/L (under no NO_3^- controls) to 23 µeq/L (under preindustrial conditions) by 2200; a decline of stream NO_3^- of 90 ueq/L. With less leaching losses of NO_3^- from soil, H^+ leaching will decrease, corresponding with increases in pH and ANC. The pH dependent algorithm for SO_4^{2-} adsorption suggests that initially under decreases in atmospheric NO_3^- deposition, increases in soil pH will drive desorption of SO_4^{2-} from soil offsetting the recovery associated with decrease in NO_3^-. In contrast, the simulations in which atmospheric NO_3^- deposition is projected to remain constant, increases in NO_3^- leaching acidify soil and enhance SO_4^{2-} adsorption. Over the course of the simulation, stream SO_4^{2-} concentrations increase as the soil comes to steady-state with atmospheric SO_4^{2-} deposition. Field studies show that the pH dependence of SO_4^{2-} adsorption/desorption is an important process controlling the recovery of GRSM watersheds. Cai et al. (2012) showed desorption of SO_4^{2-} over the pH range of 4.3–5.5 for Bw horizon soil at Noland Divide Watershed.

For simulations of controls considering a combination of SO_4^{2-} and NO_3^- decreases to preindustrial conditions, stream ANC of the study watersheds are projected to increase ranging from 21.8 µeq/L to about 121 µeq/L when the model reaches steady state around 2200. Note that MR under the combination of decreases in SO_4^{2-} and NO_3^- is much greater than under the scenarios of decreases in

SO_4^{2-} or NO_3^- individually. This relatively large increase in ANC is due the effects of decreases in NO_3^-, which delays the progression of the watersheds toward a condition of N saturation, coupled with decreases in SO_4^{2-}, which facilitates the desorption of SO_4^{2-} that had accumulated in soil under decades on elevated atmospheric SO_4^{2-} deposition. We also examined combinations of SO_4^{2-} and NO_3^- deposition that can result in a given value of ANC for all study watersheds (example shown in Figure 6 for Noland Divide Watershed). Various combinations of decreases in SO_4^{2-} and NO_3^- deposition can result in a given value of ANC, but decreases in both strong acids effectively contribute to increases in ANC.

Note that simulations suggest that the ANC of Goshen Prong does not recover to the estimated preindustrial value (ANC ~ 48 μeq/L) by 2200. The loss of ANC is due largely to soil acidification associated with the depletion of base cations from soil exchange sites. While our analysis suggests that controls on atmospheric NO_3^- deposition are more effective in facilitating increases in ANC than decreases in SO_4^{2-} deposition, to facilitate the recovery of GRSM watersheds it will be necessary to decrease concentrations of total strong acid anion concentrations in stream water by decreasing both NO_3^- and SO_4^{2-} in combination.

We also evaluated the relative effectiveness of controls on NH_4^+ deposition as compared to controls on NO_3^- deposition to increases in the ANC of streams. PnET-BGC is structured to address differences in ecosystem response to changes in NH_4^+ compared with NO_3^- deposition, because it simulates the acid-base chemistry associated with different watershed N transformations. We conducted simulations to address variations in NH_4^+ deposition for four sites; one that exhibits limited NO_3^- leaching (Lost Bottom Creek) and three that experience higher NO_3^- leaching (Noland Divide, Walker Camp Prong, Indian Camp Creek) (Table 8). Different levels of decrease in NH_4^+ and NO_3^- deposition were simulated for each site and the extent of increases in ANC in response to equivalent decreases in N deposition were evaluated (Table 8). One might expect that controls on NH_4^+ deposition to be more effective at increasing ANC, because NH_4^+ is an acidifying compound when it is assimilated by vegetation of microbes or is nitrified. For Lost Bottom Creek we found little difference between controls of NH_4^+ compared with NO_3^- deposition because both N compounds are relatively strongly assimilated within the watershed over a simulation period to 2050. In contrast, the other watersheds that exhibit elevated NO_3^- leaching show that controls on NH_4^+ deposition are more effective in increasing stream ANC than equivalent controls on NO_3^- deposition, similar to a pattern expected from ion chemistry theory. The extent of increases in ANC per equivalent decrease in NH_4^+ or NO_3^- deposition decreased over the simulation period because the watershed responded to relatively rapidly initially to controls on N deposition and response diminished over time.

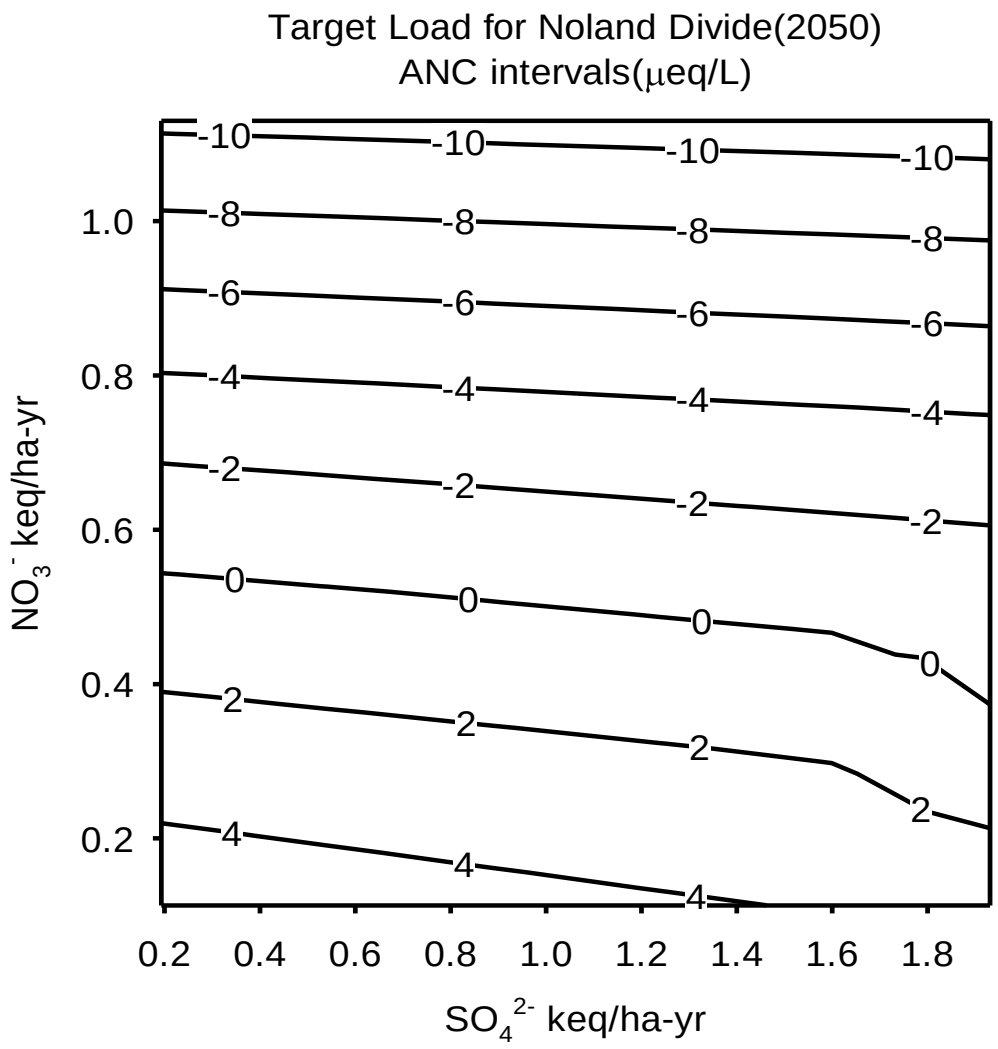

Figure 6. Isopleth map of combinations of total SO42- and NO3- deposition for Noland Divide Watershed that result in a value of ANC. Isopleth values represent ANC values in μeq/L.

Table 8. Changes in stream acid neutralizing capacity per unit equivalent decrease in ammonium and nitrate deposition for watersheds of Great Smoky Mountain National Park over the period to 2050. Note that the sites studied exhibit a different response depending on the extent of nitrate leaching.

Site Name	Volume-weighted NO_3^- (μmol/L)	$\Delta ANC/\ \Delta NH_4^+$ (μeq/L/(keq/ha-yr))	$\Delta ANC/\ \Delta NO_3^-$ (μeq/L/(keq/ha-yr))
Lost Bottom Creek	7.7	0.16	0.16
Walker Camp Prong	38	0.31	0.46
Indian Camp Creek	42.1	0.46	1.02
Noland Divide	44.3	0.31	0.36

Developing CLs/DCLs for GRSM

The correlations showing the levels of atmospheric SO_4^{2-} + NO_3^- deposition needed to achieve stream ANC targets of 0, 20 or 50 µeq/L based on model projections (Figure 1) suggest that declines in SO_4^{2-} + NO_3^- deposition will increase stream ANC across GRSM. The higher the preindustrial or current ANC, the higher the maximum level of atmospheric SO_4^{2-}+NO_3^- deposition that would allow a desired target to be met by a time period of interest. Variations in atmospheric deposition associated with variation in elevation coupled with variations in the acid sensitivity of watersheds affect the maximum acceptable deposition levels; higher elevation watersheds and soils with lower SO_4^{2-} adsorption capacity being more sensitive to acidic deposition. If a target ANC is set to be 0 µeq/L for GRSM by 2050, total SO_4^{2-}+ NO_3^- deposition maxima would range from 0.8 keq/ha-yr – 12 keq/ha-yr across the 12 modeled streams (Table 9). To achieve higher ANCs, like 20 µeq/L or 50 ueq/L, the maximum deposition of SO_4 and NO_3^- would need to be decreased to the range from 0 keq/ha-yr – 9 keq/ha-yr for an ANC of 20 µeq/L and of 0 keq/ha-yr – 5 keq/ha-yr for an ANC of 50 µeq/L. With a combined SO_4^{2-} + NO_3^- deposition of less than 1 keq/ha-yr compared to current levels of 0.6 keq/ha-yr – 3.2 keq/ha-yr, all sites simulated can obtain an ANC of 0 µeq/L by 2050 (Table 9). However simulations suggest that all the study watersheds cannot achieve 20 µeq/L by 2050, even under a condition that atmospheric S and NO_3^- were decreased to preindustrial conditions. The watersheds that *would not* achieve an ANC of 20 µeq/L by 2050 include Noland Divide (current ANC = 4.2 µeq/L), Walker Camp Prong (ANC = -13.3 µeq/L), Goshen Prong (ANC = 19.3 µeq/L) and Indian Camp Creek (ANC = 16.9 µeq/L). These sites have received elevated acidic deposition and are highly sensitive to acidic deposition (e.g., Noland Divide Watershed) or are affected by natural soil properties (i.e., Anakeesta in Walker Camp Prong; Cai et al., 2012; Grell, 2010). These sites appear to have inherently low ANC (Table 1). The soils in these watersheds are naturally low in exchangeable base cations. Moreover, acid-sensitive soils of GRSM experience exchangeable cation pools that have been depleted by historical acidic deposition, have accumulated SO_4^{2-} through adsorption, and exhibit high nitrification rates. The recovery of these sensitive and acidified watersheds will not only depend on the control of atmospheric deposition, but on inherent soil properties. Due to the internal properties, the recovery process of soils will be delayed in these watersheds, and possibly take decades or even centuries for total recovery.

To explore preexisting factors that affect acidification and recovery, we developed relationships for HA and MR with total acidic deposition, current ANC and preindustrial ANC (1850) and soil SO_4^{2-} adsorption capacity. These empirical relationships showed similar patterns. There is inherent variability in watershed ANC due to elevation, soil characteristics and land disturbance history that influences the sensitivity to acidic deposition and the response to decreased deposition. In addition, the watersheds clearly show variation in the historical acidification and recovery that are driven by the magnitude of acidic deposition and subsequent decreases in deposition. In GRSM, deposition of SO_4^{2-} and NO_3^- varies by elevation and total SO_4^{2-} deposition closely corresponds with total NO_3^- deposition. Cai et al. (2010) also showed that acidification in Noland Divide Watershed was strongly dependent on current total SO_4^{2-} + NO_3^- deposition.

Table 10 shows all simulated watersheds showing projected values in pH and ANC by 2040 that would occur under a hypothetical decrease in SO_4^{2-} + NO_3^- deposition of 60%. This is thought be a

reasonable scenario of decreases in deposition that could occur in future years. Simulated pH and ANC are compared to current (2006) values and hindcast projections of preindustrial values. These simulations show the diverse response of watersheds to a hypothetical projection of decreases in acidic deposition. None of the watersheds are simulated to recover to historical values of ANC. Some watersheds are projected to increase in ANC from current values (Goshen Prong, Lost Bottom Creek, Left Prong Anthony, Pretty Hollow, Cannon Creek, Thunderhead, Mill Creek), while other are projected to continue loss of ANC largely due to increasing leaching losses of NO_3^- associated with approaching a condition of N saturation (Noland Divide, Indian Camp Creek, Walker Camp Prong, Cosby Creek, Sugar Fork).

Table 9. Dynamic critical loads (DCL) of NO3- + SO42 deposition necessary to reach ANC targets at various time steps based upon PnET-BGC model forecasts for 12 study stream within Great Smoky Mountains National Park. Simulated pre-industrial ANC, current 2010 ANC, current deposition of NO_3^- + SO_4^{2} and TDEC target ANC's are provided for comparative purposes. Target ANCs were generated for study streams that did not have TDEC targets using the technique similar to the methods described in TDEC (2010). Note N/A represents time steps and ANC targets that are not attainable based upon current conditions and forecasted model simulations.

Stream	Pre-Industrial ANC*	Current ANC*	Current SO_4 Dep**	Current NO^3 Dep**	TDEC ANC Target*	2050 DCL ANC=0	2100 DCL ANC=0	2200 DCL ANC=0	2050 DCL ANC=20	2100 DCL ANC=20	2200 DCL ANC=20	2050 DCL ANC=50	2100 DCL ANC=50	2200 DCL ANC=50
Noland Divide	40	4.31	1.82	1.02	22.0	1.30	0.76	0.40	N/A	N/A	N/A	N/A	N/A	N/A
Indian Camp Creek	65.6	16.9	1.88	0.78	17.17	1.33	0.99	0.73	0.41	0.53	0.26	N/A	N/A	N/A
Walker Camp Prong	41	-13.3	1.8	2.9	6.52	0.27	0.18	0.10	N/A	N/A	N/A	N/A	N/A	N/A
Goshen Prong	58.9	11.2	0.5	1.7	17.84	0.85	0.51	0.36	0.32	0.28	0.16	N/A	N/A	N/A
Lost Bottom Creek	90	58.7	0.56	0.95	57.31	2.24	1.36	0.82	1.58	0.98	0.58	0.60	0.41	0.23
Left Prong Anthony	81.6	40	0.81	1.05	25.60	1.42	1.39	1.00	0.96	0.71	N/A	0.27	0.22	N/A
Pretty Hollow	84.8	51	0.48	1.00	29.90	3.37	2.08	1.34	2.32	1.47	0.94	0.74	0.55	0.34
Cosby Creek	93.1	43.7	1.04	1.43	36.62	2.00	1.30	1.20	1.11	0.82	0.46	N/A	N/A	N/A
Sugar Fork	107.1	87.5	0.69	0.31	70.53	2.97	2.12	1.51	2.34	1.71	1.22	1.40	1.10	0.78
Cannon Creek	60.5	14.4	1.13	1.43	18.65	1.76	1.15	0.78	0.77	0.64	0.46	N/A	N/A	N/A
Thunderhead	73.3	30.7	0.76	1.44	19.59	2.77	1.81	1.05	1.65	1.14	0.70	N/A	N/A	N/A
Mill Creek	92.9	45.8	0.69	1.6	49.40	2.25	1.46	0.94	1.57	1.05	0.68	0.56	0.44	0.30

Note: *(μeq/L) **(keq/ha-yr)

Table 10. Projected streamwater ANC for twelve GRSM modeled watersheds under pre-industry time; Streamwater ANC, pH under current deposition scenario compared with streamwater pH, ANC in 2040 under 60% reduction scenario

Site	Pre-Industrial ANC* Streamwater (µeq/L)	Total NO_3 + SO_4^{2-} Deposition 2006 (keq/ha-yr)	Streamwater ANC* 2006 (µeq/L)	Streamwater pH 2006	NO_3 + SO_4^{2-} 2040 assuming 60% reduction** from 2008 N/S deposition (keq/ha-yr)	ANC 2040 assuming 60% reduction** from 2008 N/S deposition (µeq/L)	pH 2040 assuming 60% reduction** from 2008 N/S deposition
Noland Divide	40	2.87	4.31	5.8	1.02	1.3	5.7
Indian Camp Creek	65.6	2.56	16.9	6	0.96	4	5.4
Walker Camp Prong	41	3.47	-13.3	4.8	1.70	-14.7	4.7
Goshen Prong	58.9	2.21	11.2	6.1	0.79	12	5.7
Lost Bottom Creek	90	1.00	58.7	6.5	0.54	60	6.4
Left Prong Anthony	81.6	1.26	40	6.3	0.67	46	6.3
Pretty Hollow	84.8	1.12	51	6.4	0.53	54.7	6.4
Cosby Creek	93.1	1.57	43.7	6.3	0.89	26.7	6
Sugar Fork	107.1	0.61	87.5	6.5	0.36	83	6.3
Cannon Creek	60.5	2.08	14.4	5.9	0.92	19.1	5.9
Thunderhead	73.3	1.75	30.7	6.2	0.79	37	6.2
Mill Creek	92.9	1.78	45.8	6.4	0.82	52.3	6.3

*Values for ANC Pre-Industrial and ANC 2006 copied from Table 9 in draft report
** The 60% reduction in N/S would occur from 2008–2020.

5. Conclusions

Simulations were conducted with the biogeochemical model PnET-BGC to 12 stream watersheds in GRSM, including two streams that are listed as impaired by the State of Tennessee due to elevated acidity (pH >6). The objective of this study was to examine past and potential future response to changes in atmospheric SO_4^{2-} and NO_3^- deposition. We used the results of simulations of hypothetical future decreases in atmospheric NO_3^- and SO_4^{2-} deposition to pre-industrial values to evaluate the potential recovery of sensitive watersheds and their CLs and DCLs of acidity. PnET-BGC is able to simulate current stream chemistry and watershed biogeochemical processes at GRSM. Hindcast simulations suggest that historical atmospheric deposition resulted in marked increases in stream SO_4^{2-} (Δ 26 µeq/L) and NO_3^- (Δ 22 µeq/L), resulting in decreases in the pH (Δ -0.6) and ANC (Δ – 37 µeq/L). The extent of changes in stream chemistry in response to changes in atmospheric deposition is largely driven by watershed variability across GRSM, associated with elevation, variations in acid deposition, historical land disturbance and soil characteristics. We observed a relationship between historical acidification and potential watershed recovery with changes in $NO_3^- + SO_4^{2-}$ deposition and historical ANC (1850). Stream ANC in GRSM watersheds increases to a greater extent in response to decreases in NO_3^- deposition than to decreases in SO_4^{2-} deposition. Decreases in NO_3^- deposition to GRSM watersheds increases desorption of previously absorbed soil SO_4^{2-}, which delays recovery. A relationship exists between current ANC and the level of deposition needed to achieve a target ANC. This relationship could be utilized with stream survey data for GRSM to develop a Park-wide TMDL or CL/DCL.

6. Literature Cited

Aber, J.D., and Driscoll, C.T. (1997). Effects of land use, climate variation, and N deposition on N cycling and C storage in northern hardwood forests. Glob. Biogeochem. Cycles *11*, 639–648.

Aber, J.D., Ollinger, S.V., and Driscoll, C.T. (1997). Modeling nitrogen saturation in forest ecosystems in response to land use and atmospheric deposition. Ecol. Model. *101*, 61–78.

Aber, J.D., Goodale, C.L., Ollinger, S.V., Smith, M.-L., Magill, A.H., Martin, M.E., Hallett, R.A., and Stoddard, J.L. (2003). Is nitrogen deposition altering the nitrogen status of northeastern forests? BioScience *53*, 375–389.

Baron, J.S., Driscoll, C.T., Stoddard, J.L., and Richer, E. (2011). Empirical critical loads of atmospheric nitrogen deposition for nutrient enrichment and acidification of sensitive US lakes. BioScience *61*, 602–613.

Burns, D.A., Blett, T., Haeuber, R., and Pardo, L.H. (2008). Critical loads as a policy tool for protecting ecosystems from the effects of air pollutants. Front. Ecol. Environ. *6*, 156–159.

Cai, M., and Schwartz, J.S. (2012). Biological Effects of Stream Water Quality on Aquatic Macroinverterbrates and Fish Communities within Great Smoky Mountains National Park. A draft report for Great Smoky Mountains National Park.

Cai, M., Robinson, R.B., Moore, S.E., and Kulp, M.A. (2010). Long-term Acid Deposition Effects on Soil and Water Chemistry in the Noland Divide Watershed, Great Smoky Mountains National Park, USA. Water. Air. Soil Pollut. *209*, 143–156.

Cai, M., Johnson, A.M., Schwartz, J.S., Moore, S.E., and Kulp, M.A. (2012). Soil acid-base chemistry of a high-elevation forest watershed in the Great Smoky Mountains National Park: influce of acidic deposition. Water. Air. Soil Pollut. *223*, 289–303.

Chen, L., and Driscoll, C.T. (2004). An evaluation of processes regulating spatial and temporal patterns in lake sulfate in the Adirondack region of NY. Glob. Biogeochem. Cycles *18 :GB3024*.

Chen, L., and Driscoll, C.T. (2005). Regional application of an integrated biogeochemical model to northern New England and Maine. Ecol. Appl. *15*, 1783–1797.

Church, M.R., Thornton, K.W., Shaffer, P.W., Stevens, D.L., Rochelle, B.P., Holdren, G.R., Johnson, M.G., Lee, J.J., Turner, R.S., Cassel, D.L., et al. (1989). Future effects of long-term sulfur deposition on surface water chemistry in the Northeast and Southern Blue Ridge Province: Results of the DDRP. EPA/600/3-89/061, United States Environmental Protection Agency, Corvallis, OR.

Cook, R.B., Elwood, J.W., Turner, R.R., Bogle, M.A., Mulholland, P.J., and Palumbo, A.V. (1994). Acid-base chemistry of high-elevation streams in the Great Smoky Mountains. Water. Air. Soil Pollut. *72*, 331–356.

Driscoll, C.T., Lawrence, G.B., Bulger, A.J., Butler, T.J., Cronan, C.S., Eagar, C., Lambert, K., Likens, G.E., Stoddard, J.L., and Weathers, K.C. (2001). Acidic deposition in the Northeastern United States: Sources and Inputs, Ecosystem Effects, and Mgmt. Strategies. BioScience *51*.

Elwood, J.W., Sale, M.J., Kaufmann, P.R., and Cada, G.F. (1991). The Southern Blue Ridge Province. In Acidic Deposition and Aquatic Ecosystems. Regional Case Studies, D.F. Charles, ed. (New York: Springer-Verlag), pp. 319–364.

Flum, T., and Nodvin, S. (1995). Factors affecting streamwater chemistry in the Great Smoky Moutains, USA. Water. Air. Soil Pollut. *85*, 1707–1712.

Gbondo-Tugbawa, S.S., and Driscoll, C.T. (2002). Evaluation of the effects of future controls on sulfur dioxide and nitrogen oxide emissions on the acid-base status of a northern forest ecosystem. Atmos. Environ. *36*, 1631–1643.

Gbondo-Tugbawa, S.S., Driscoll, C.T., Aber, J.D., and Likens, G.E. (2001). Evaluation of an integrated biogeochemical model (PnET-BGC) at a northern hardwood forest ecosystem. Water Resour. Res. *37*, 1057–1070.

Goodale, C.L., and Aber, J.D. (2001). The long-term effects of land-use history on nitrogen cycling in northern hardwood forests. Ecol. Appl. *11*, 253–267.

Grell, M.. (2010). Soil Chemistry characterization of acid sensitive watersheds in Great Smoky Mountains National Park. Ph.D. Dissertation. The University of Tennessee, Knoxville.

Ito, M., Mitchell, M.J., and Driscoll, C.T. (2002). Spatial patterns of precipitation quantity and chemistry and air temperature in the Adirondack region of New York. Atmos. Environ. *36*, 1051–1062.

Janssen, P.H.M., and Heuberger, P.S.C. (1995). Calibration of process-oriented models. Ecol. Model. *83*, 55–66.

Johnson, D.W., and Lindberg, S.E. (1992). Atmospheric Deposition and Forest Nutrient Cycling: A Synthesis of the Integrated Forest Study. (New York: Springer-Verlag).

Kahl, J.S., Stoddard, J.L., Haeuber, R., Paulsen, S.G., Birnbaum, R., Deviney, F.A., Webb, J.R., DeWalle, D.R., Sharpe, W., Driscoll, C.T., et al. (2004). Have U.S. surface waters responded to the 1990 Clean Air Act Amendments? Environ. Sci. Technol. *38*, 484A–490A.

Lehmann, C., Bowersox, V., and Larson, S. (2005). Spatial and temporal trends of precipitation chemistry in the United States, 19850-2002. Environ. Pollut. *135*, 347–361.

Lovett, G.M., Bowser, J.J., and Edgerton, E.S. (1997). Atmospheric deposition to watersheds in complex terrain. Hydrol. Process. *11*, 645–654.

McNulty, S.G., Cohen, E.C., Myers, J.A.M., Sullivan, T.J., and Li, H. (2007). Estimates of critical acid loads and exceedances for forest soils across the conterminous United States. Environ. Pollut. *149*, 281–292.

Moore, P.T., Van Miegroet, H., and Nicholas, N.S. (2008). Examination of forest recovery scenarios in a southern Appalachian Picea-Abies forest. Forestry *81*, 183–194.

Neff, K.J., Schwartz, J.S., Henry, T.B., Robinson, R.B., Moore, S.E., and Kulp, M.A. (2009). Physiological stress in native southern brook trout during episodic stream acidification in the Great Smoky Mountains National Park. Arch. Environ. Contam. Toxicol. *10.1007/s00244-008-9269-4: 57*, 366–376.

Neff, K.J., Schwartz, J.S., Moore, S.E., and Kulp, M.A. (2013). Influence of basin characteristics on episodic stream acidification in the Great Smoky Mountains National Park, USA. Hydrol. Proc. *27,* 2061-2074. DOI 10.1002/hyp.9366.

Nicholas, N.S., and Zedaker, S.M. (1989). Ice damage in Spruce fir forests of he Black Mountains, North Carolina. Can. J. Forest Res. *19*, 1487–1491.

Nilsson, J., and Grennfelt, P. (1988). Critical Loads for Sulphur and Nitrogen. UNECE/Nordic Council workshop report, Skokloster, Sweden. March 1988. Nordic Council of Ministers: Copenhagen. 418 pp.

Nodvin, S.C., Van Miegroet, H., Lindberg, S.E., Nicholas, N.S., and Johnson, D.W. (1995). Acidic deposition, ecosystem processes, and nitrogen saturation in a high elevation Southern Appalachian Watershed. Water. Air. Soil Pollut. *85*, 1647–1652.

Ollinger, S.V., Aber, J.D., Lovett, G.M., Millham, S.E., Lathrop, R.G., and Ellis, J.M. (1993). A spatial model of atmospheric deposition for the northeastern U S. Ecol. Appl. *3*, 459–472.

Pardo, L.H. (2010). Approaches for estimating critical loads of N and S deposition for forest ecosystems on U.S. federal lands. Gen. Technical Rep. NRS-71 USDA For. Serv. North. Res. Stn. Newtown Sq. Pa. USA.

Pardo, L.H., Fenn, M., Goodale, C.L., Geiser, L.H., Driscoll, C.T., Allen, E., Baron, J., Bobbink, R., Bowman, W.D., Clark, C., et al. (2011). Effects of nitrogen deposition and empirical nitrogen critical loads for ecoregions of the United States. Ecol. Appl. *21*, 3049–3082.

Porter, E., Blett, T., Potter, D.U., and Huber, C. (2005). Protecting resources on federal lands: Implications of critical loads for atmospheric deposition of nitrogen and sulfur. Bioscience *55*, 603–612.

Pourmokhtarian, A., Driscoll, C.T., Campbell, J.L., and Hayhoe, K. (2012). Modeling potential hydrochemical responses to climate change and rising CO_2 at the Hubbard Brook Experimental Forest using a dynamic biogeochemical model (PnET-BGC). Water Res. Res. *48, W07514*, 13pp.

Pyle, C. (1985). Vegetation disturbance history of Great Smoky Mountains National Park: An analysis of archival maps and records. NPS.-Southeast Reg. Res. Manag. Rep. SER-77.

Robinson, R.B., Barnett, T.W., Harwell, G.R., Moore, S.E., Kulp, M., and Schwartz, J.S. (2008). pH and acid anion time trends in different elevation ranges in the Great Smoky Mountains National Park. J. Environ. Eng.-ASCE *134*, 800–808.

Schwartz, J.S., Cai, M., Neff, K.J., Moore, S.E., and Kulp, M.A. (2012). Great Smoky Mountains National Park, Summary Water Quality Report. Prepared for the US Dept. of Interior, National Park Service. University of Tennessee-Knoxville, Department of Civil and Environmental Engineering. June 2012.

Shannon, J.D. (1981). A model of regional long-term average sulfur atmospheric pollution, surface removal, and net horizontal flux. Atmos. Environ. *15*, 689–701.

Shubzda, J., Lindberg, S.E., Garten, C.T., and Nodvin, S.C. (1995). Elevational trends in the fluxes of sulphur and nitrogen in throughfall in the southern Appalachian mountains: some surprising results. Water. Air. Soil Pollut. *85*, 2265–2270.

Smith, G.F., and Nicholas, N.S. (2000). Size and age class distributions of Fraser fir following balsam woolly adelgid infestation. Can. J. For. Res. *30*, 948–957.

Sullivan, T.J., Cosby, B.J., Driscoll, C.T., McDonnell, T.C., Herlihy, A.T., and Burns, D.A. (2012). Target loads of atmospheric sulfur and nitrogen deposition for protection of acid sensitive aquatic resources in the Adirondack Mountains, New York. Water Resour. Res. *48, W01547*, 16pp.

TDEC (2010). Proposed Total Maximum Load (TMDL) for low pH in the Great Smoky Mountains National Park located in the Pigeon River Watershed (HUC 06010106) Lower French Broad River Watershed (HUC 06010107) Watts Bar Lake Watershed (HUC 06010201) Cocke and Sevier County, Tennessee (Prepared by Tennessee Department of Environment and Conservation Division of Water Pollution Control).

USEPA (2009). Risk and Exposure Assessment for Review of the Secondary National Ambient Air Quality Standards for Oxides of Nitrogen and Oxides of Sulfur. EPA-452/P-09-004a.

Weathers, K.C., Simkin, S.M., Lovett, G.M., and Lindberg, S.E. (2006). Empirical modeling of atmospheric deposition in mountainous landscapes. Ecol. Appl. *16*, 1590–1607.

White, P.S., and Cogbill, C.V. (1992). Spruce fir forests of eastern North America. In Ecology and Decline of Red Spruce in the Eastern United States (New York: Springer-Verlag).

Zhai, J., Driscoll, C.T., Sullivan, T.J., and Cosby, B.J. (2008). Regional application of the PnET-BGC model to assess historical acidification of Adirondack lakes. Water Resour. Res. *44*.

7. Appendix 1: Time Series of Stream

Time series of stream SO_4^{2-}, NO_3^-, Ca^{2+}, ANC and pH for 12 study watersheds (y-axis) that include hindcasts and future projections to atmospheric deposition decreases in: (a) NO_3^- only, (b) SO_4^{2-} only, and (c) both NO_3^- and SO_4^{2-}. Also shown are measured values.

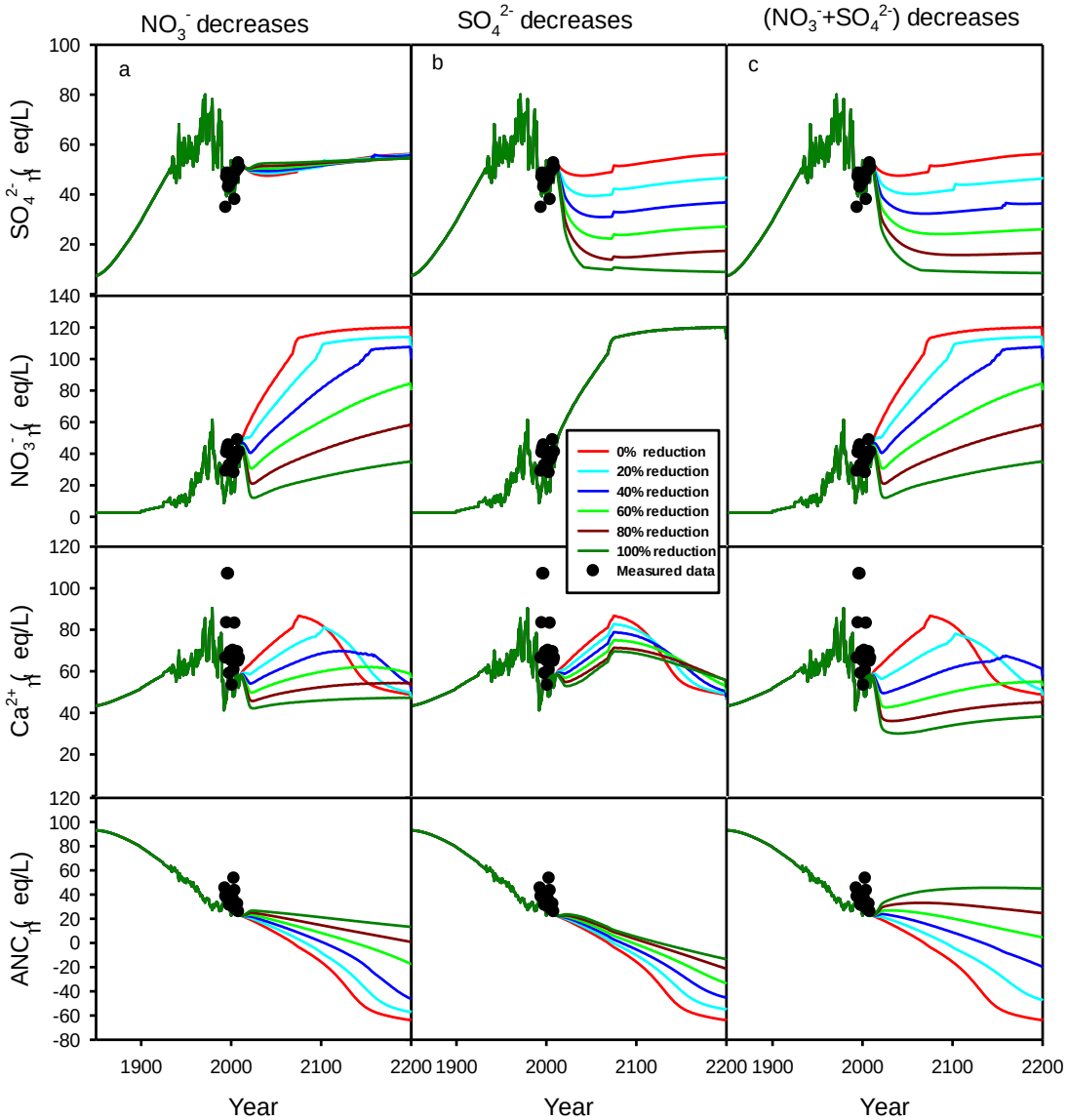

Time series of SO_4^{2-}, NO_3^-, Ca^{2+} and ANC for Cosby Creek that include hindcast and future projections to atmospheric deposition decreases in a) NO_3^- only; b) SO_4^{2-} only; c) combination of (NO_3^- + SO_4^{2-}). Also shown are measured values.

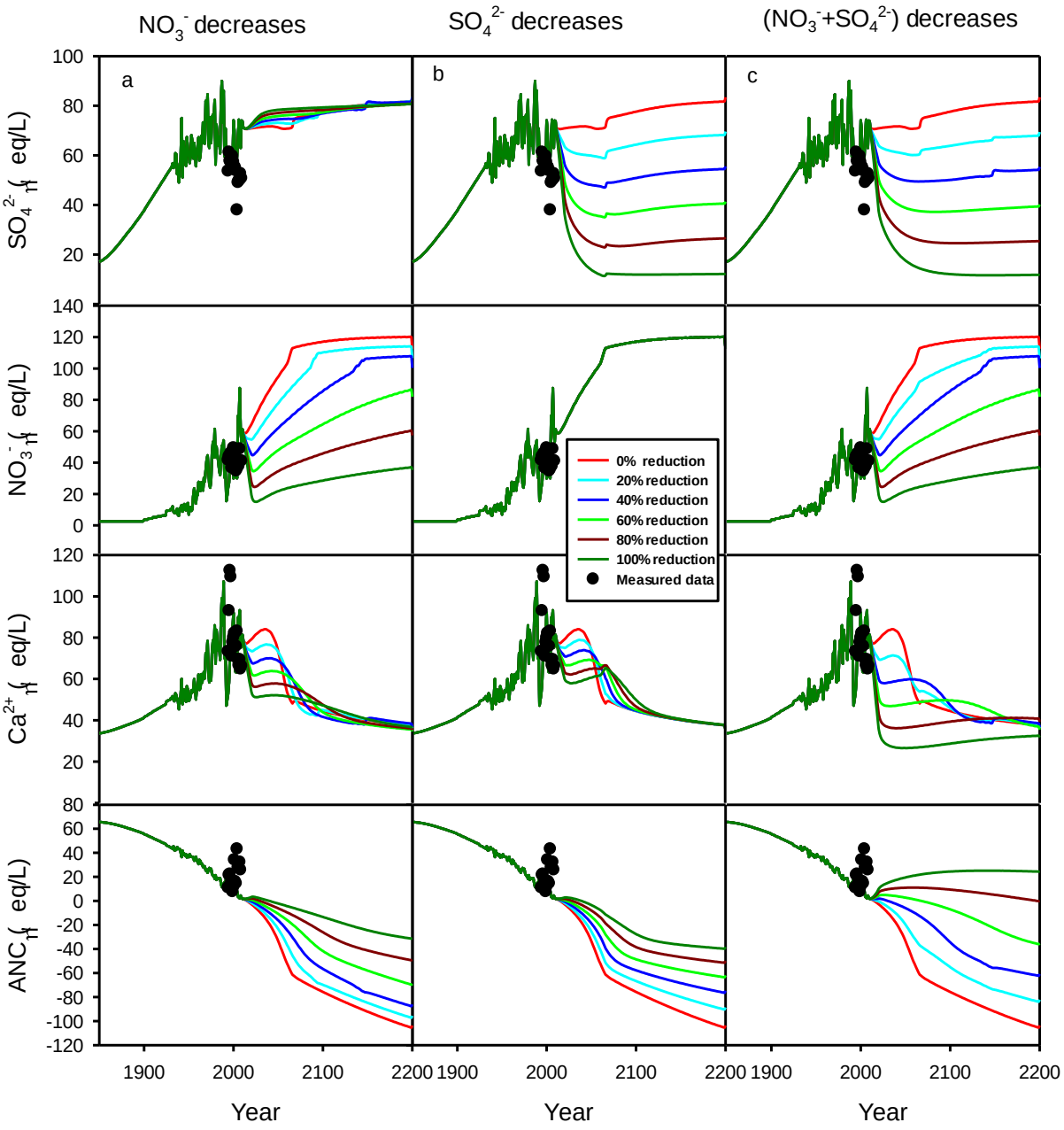

Time series of SO_4^{2-}, NO_3^-, Ca^{2+} and ANC for Indian Camp Creek that include hindcast and future projections to atmospheric deposition decreases in a) NO_3^- only; b) SO_4^{2-} only; c) Combination of (NO_3^- + SO_4^{2-}). Also shown are measured values.

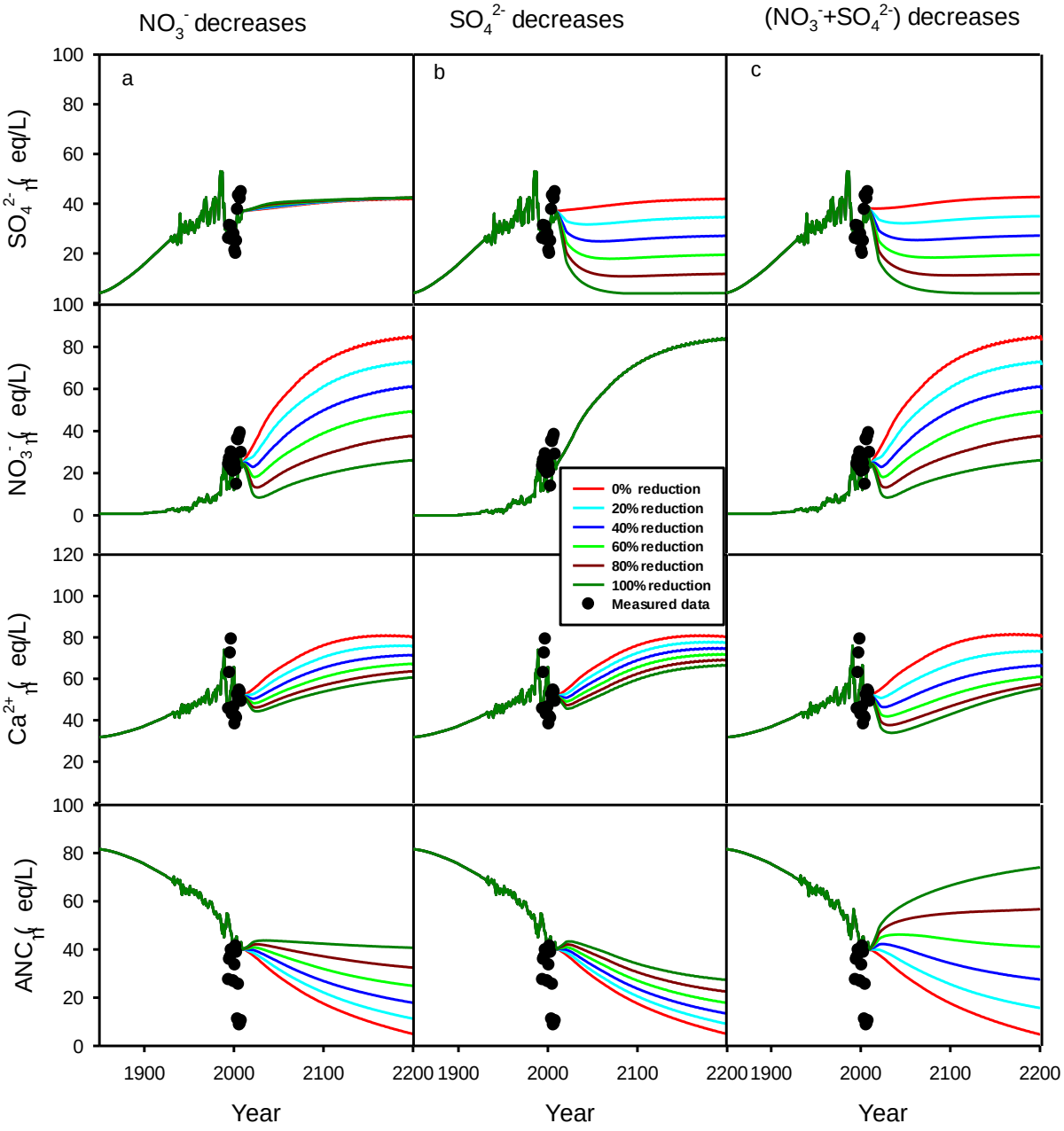

Time series of SO_4^{2-}, NO_3^-, Ca^{2+} and ANC for Left Prong Anthony that include hindcast and future projections to atmospheric deposition decreases in a) NO_3^- only; b) SO_4^{2-} only; c) Combination of (NO_3^- + SO_4^{2-}). Also shown are measured values.

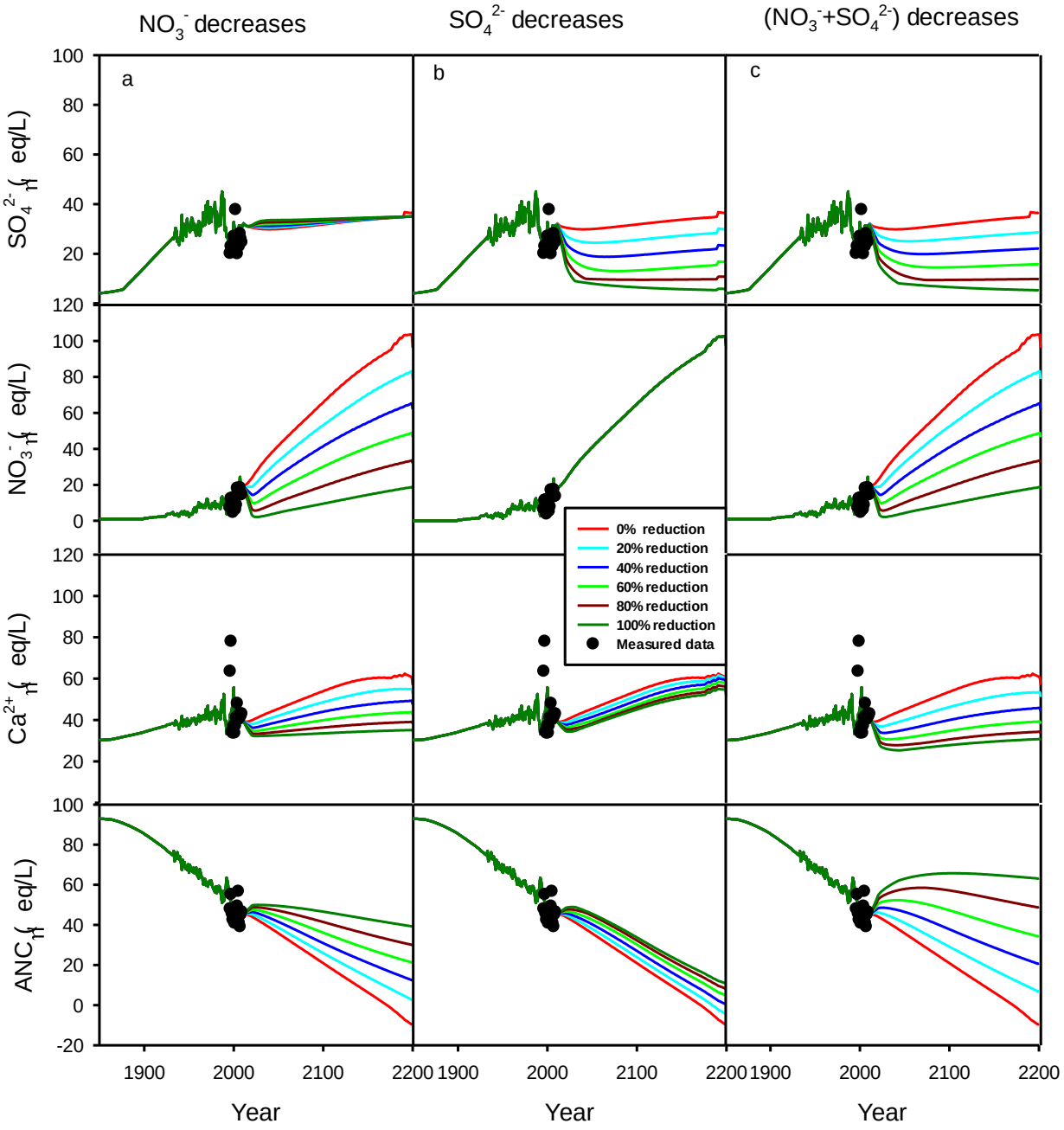

Time series of SO_4^{2-}, NO_3^-, Ca^{2+} and ANC for Mill Creek that include hindcast and future projections to atmospheric deposition decreases in a) NO_3^- only; b) SO_4^{2-} only; c) combination of (NO_3^- + SO_4^{2-}). Also shown are measured values.

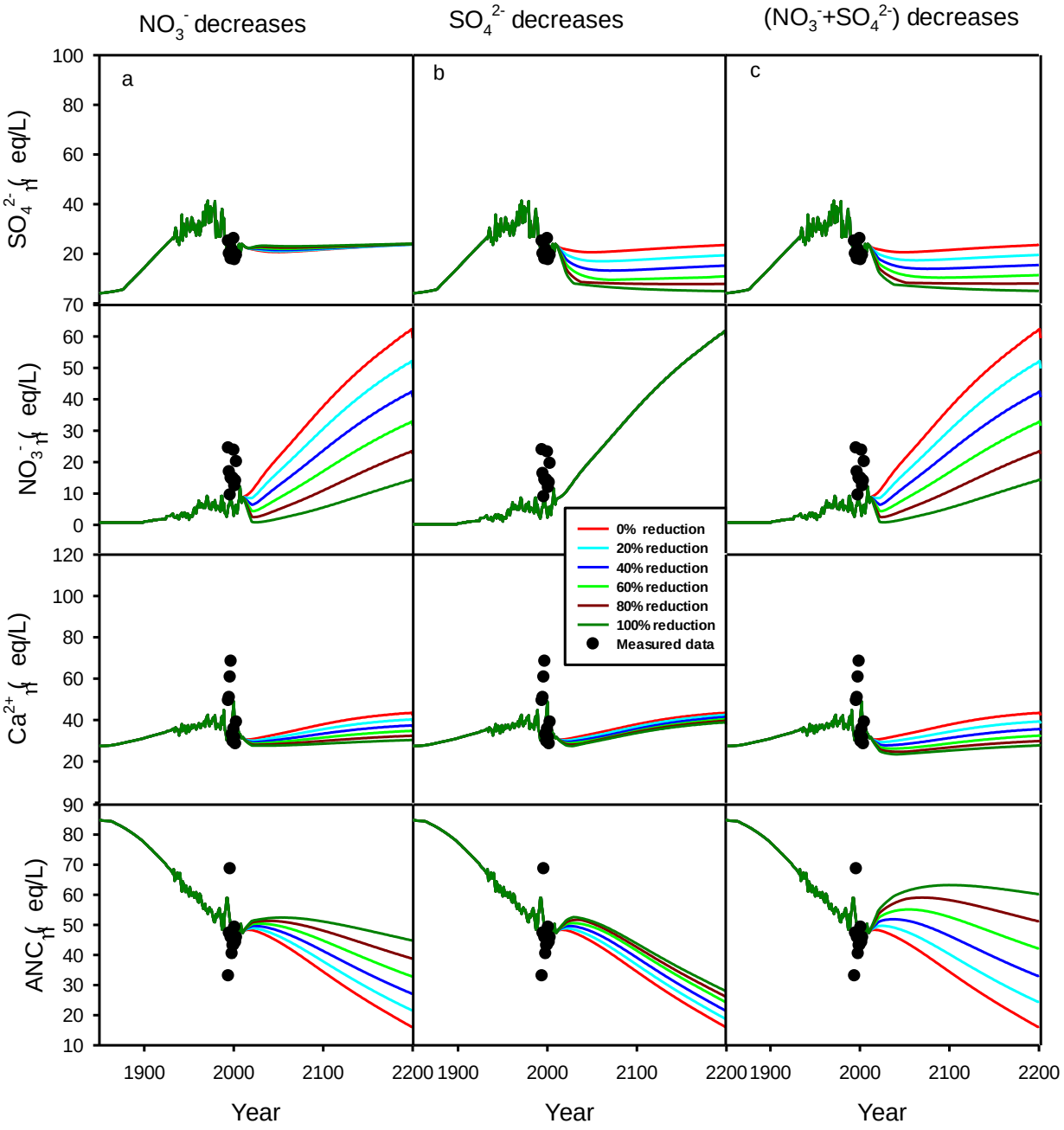

Time series of SO_4^{2-}, NO_3^-, Ca^{2+} and ANC for Pretty Hollow that include hindcast and future projections to atmospheric deposition decreases in a) NO_3^- only; b) SO_4^{2-} only; c) combination of (NO_3^- + SO_4^{2-}). Also shown are measured values.

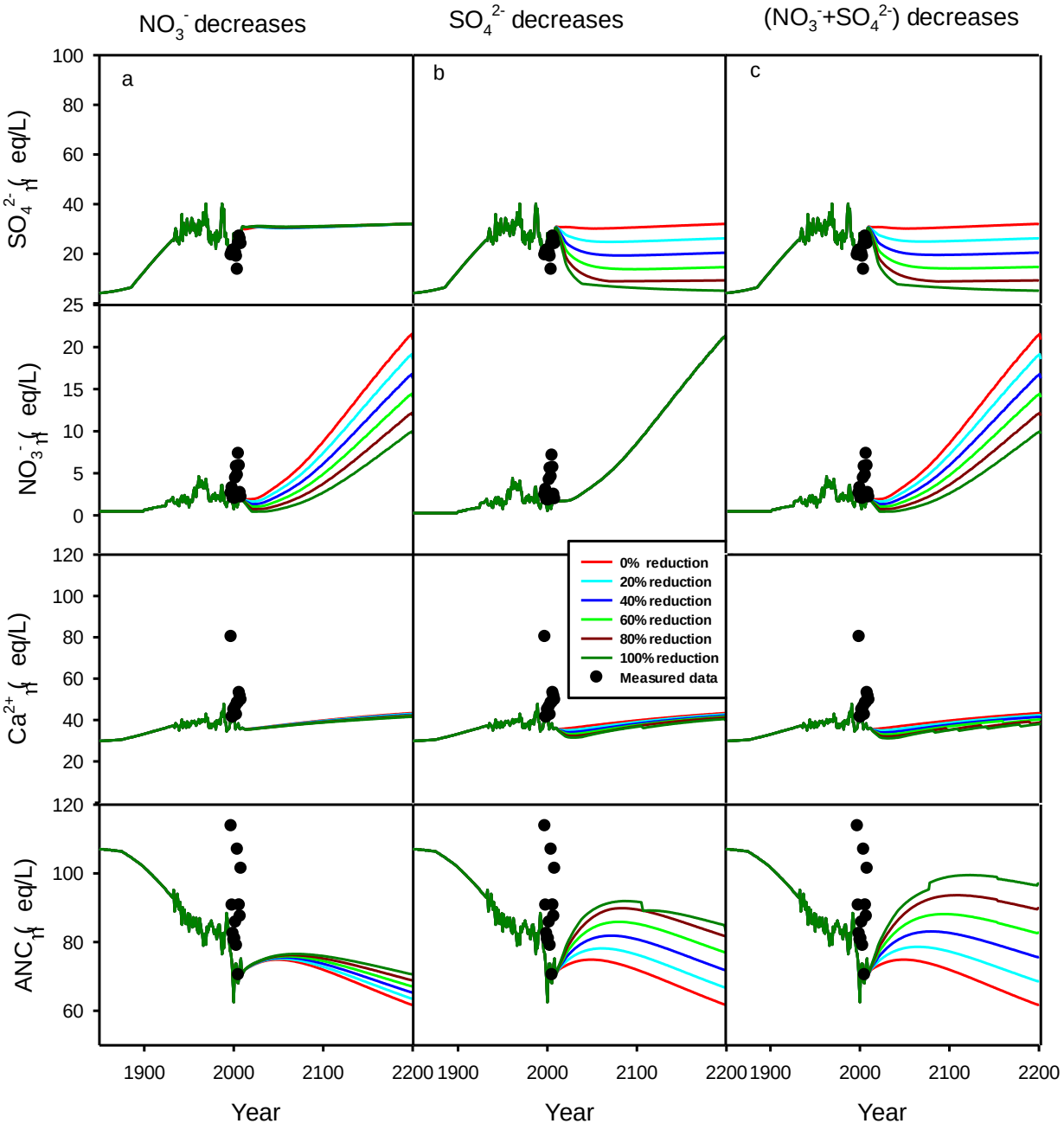

Time series of SO_4^{2-}, NO_3^-, Ca^{2+} and ANC for Sugar Fork that include hindcast and future projections to atmospheric deposition decreases in a) NO_3^- only; b) SO_4^{2-} only; c) Combination of (NO_3^- + SO_4^{2-}). Also shown are measured values.

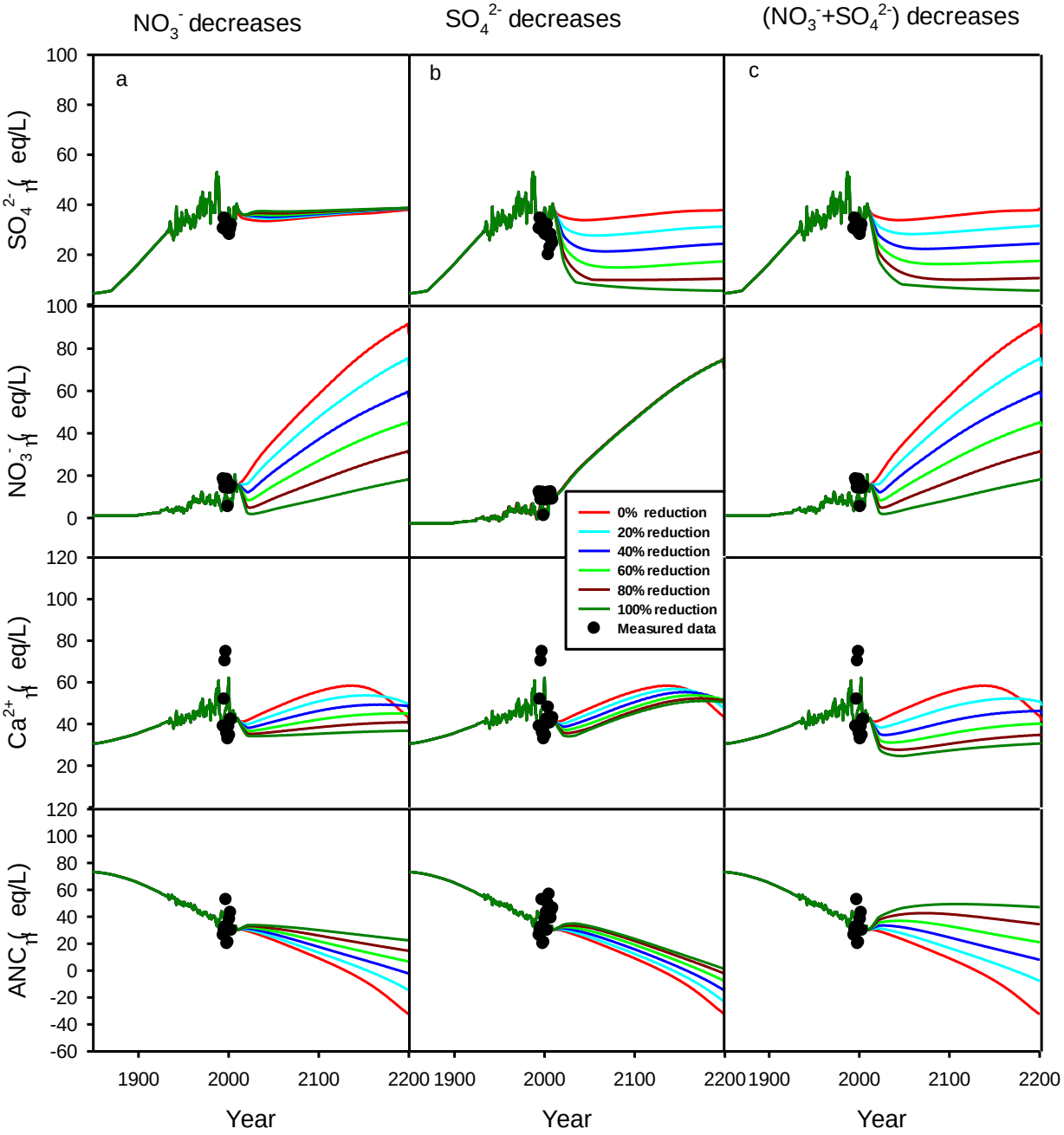

Time series of SO_4^{2-}, NO_3^-, Ca^{2+} and ANC for Thunderhead that include hindcast and future projections to atmospheric deposition decreases in a) NO_3^- only; b) SO_4^{2-} only; c) combination of (NO_3^- + SO_4^{2-}). Also shown are measured values.

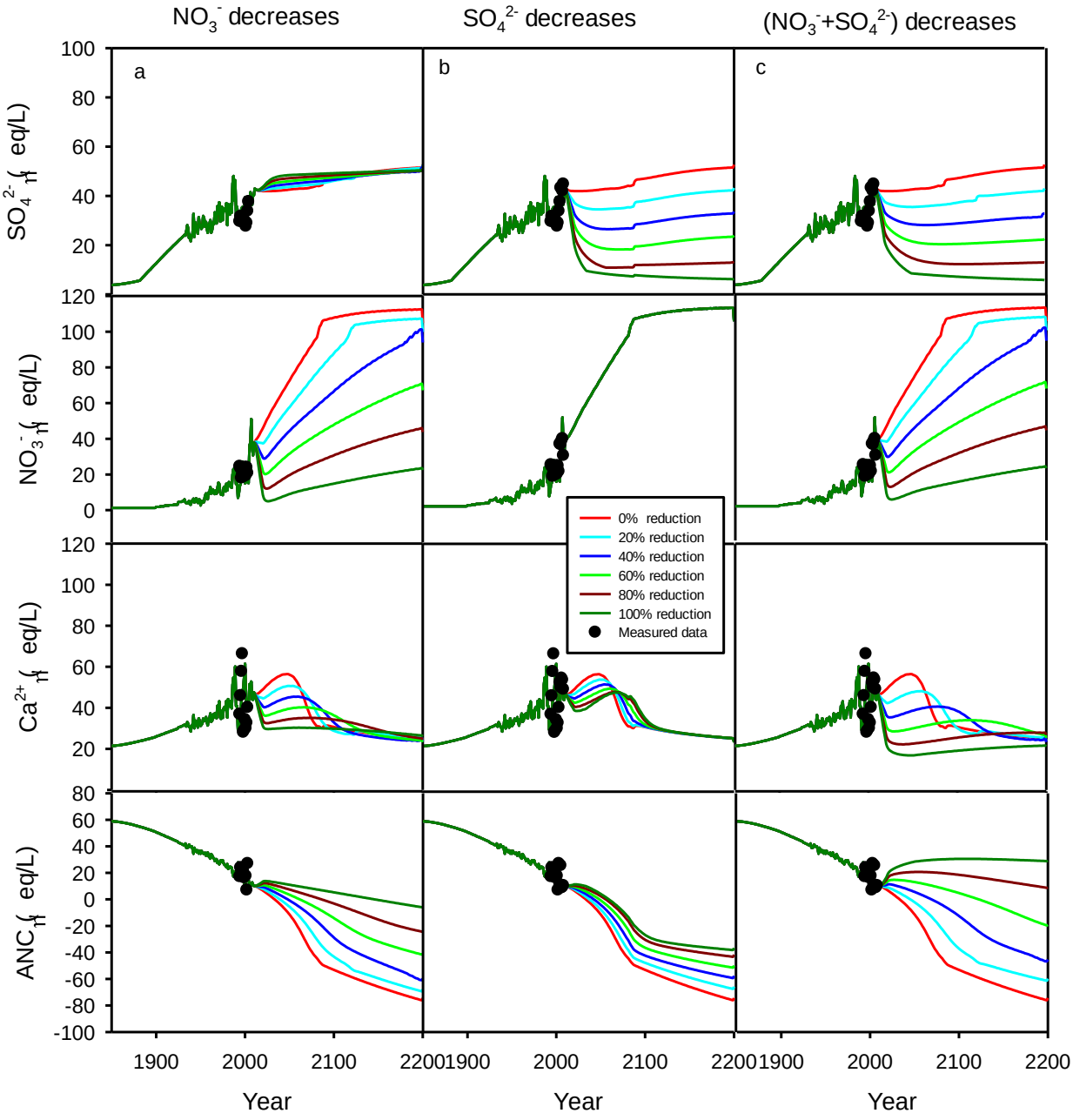

Time series of SO_4^{2-}, NO_3^-, Ca^{2+} and ANC for Goshen Prong that include hindcast and future projections to atmospheric deposition decreases in a) NO_3^- only; b) SO_4^{2-} only; c) Combination of (NO_3^- + SO_4^{2-}). Also shown are measured values.

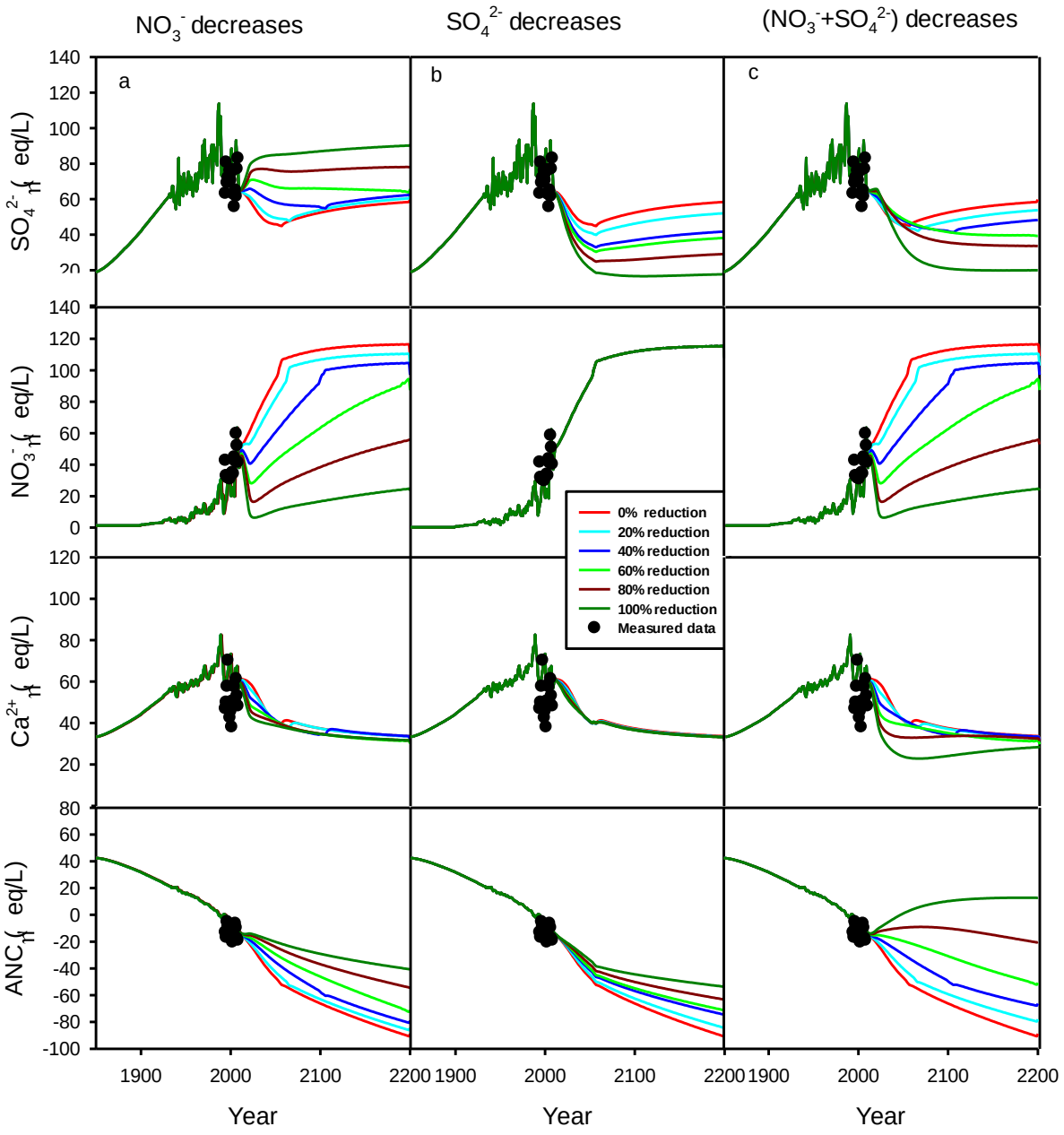

Time series of SO_4^{2-}, NO_3^-, Ca^{2+} and ANC for Walker Camp Prong that include hindcast and future projections to atmospheric deposition decreases in a) NO_3^- only; b) SO_4^{2-} only; c) combination of (NO_3^- + SO_4^{2-}). Also shown are measured values.

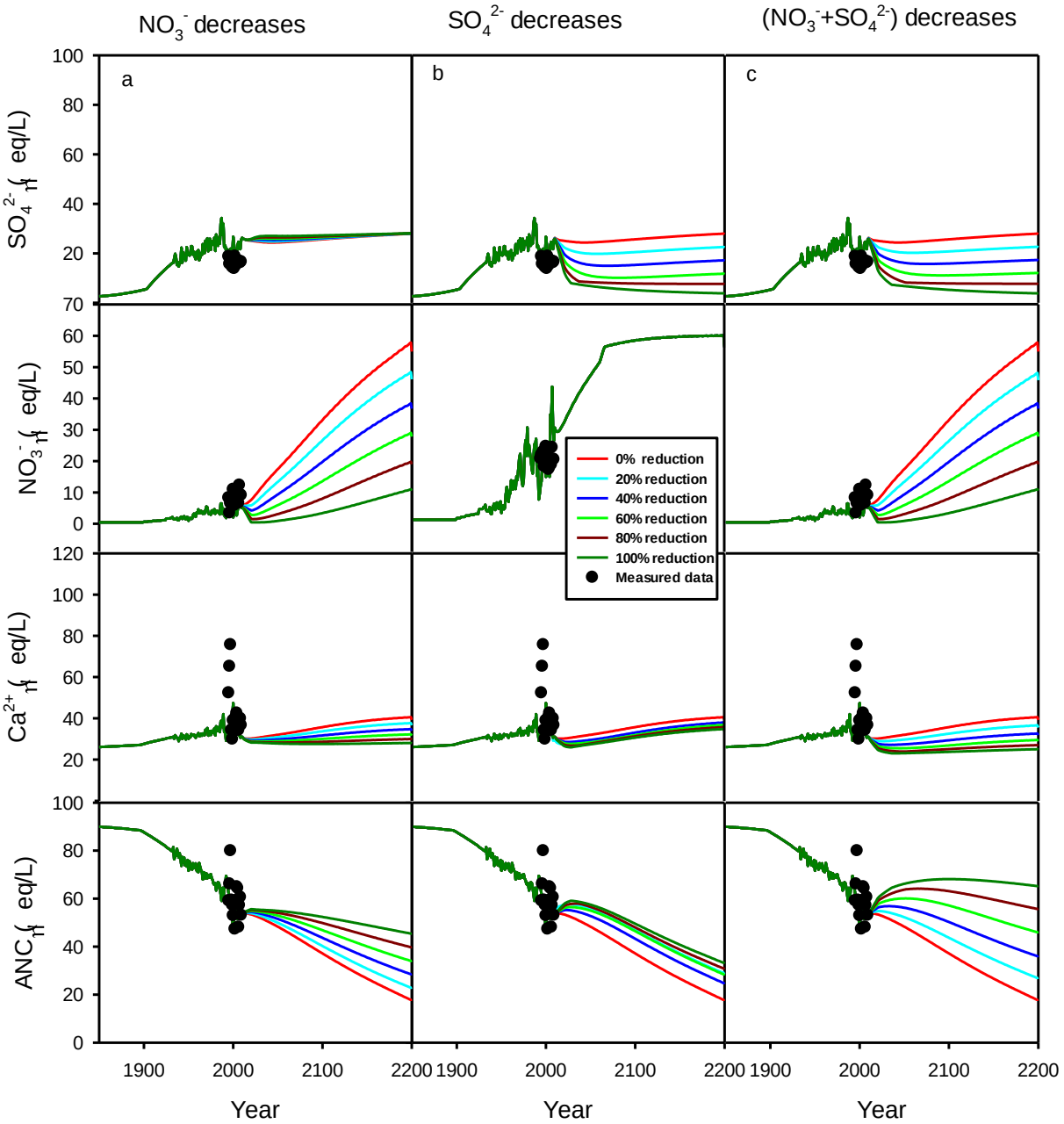

Time series of SO_4^{2-}, NO_3^-, Ca^{2+} and ANC for Lost Bottom Creek that include hindcast and future projections to atmospheric deposition decreases in a) NO_3^- only; b) SO_4^{2-} only; c) combination of (NO_3^- + SO_4^{2-}). Also shown are measured values.

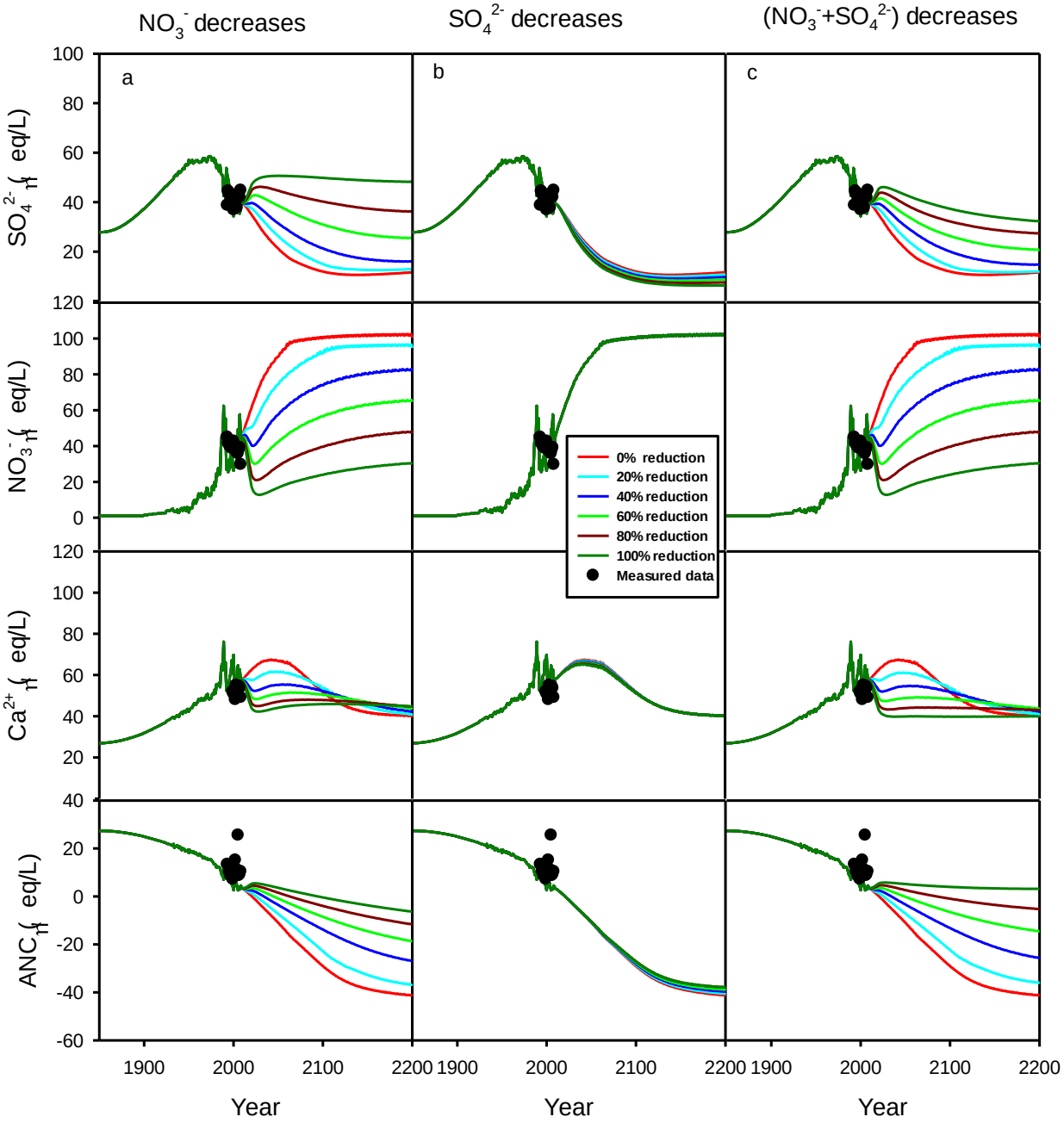

Time series of SO_4^{2-}, NO_3^-, Ca^{2+} and ANC for Noland Divide that include hindcast and future projections to atmospheric deposition decreases in a) NO_3^- only; b) SO_4^{2-} only; c) combination of (NO_3^- + SO_4^{2-}). Also shown are measured values.

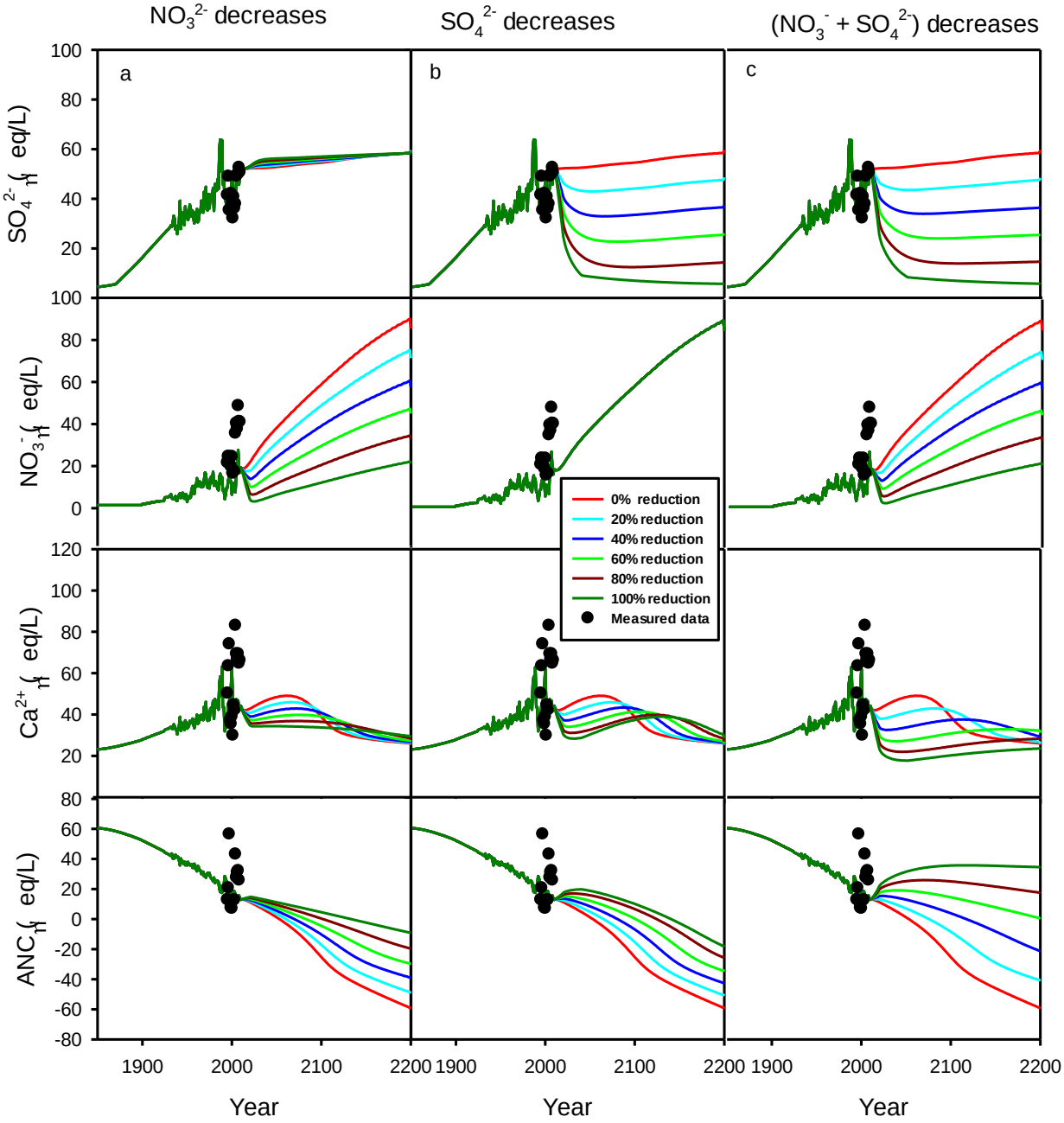

Time series of SO_4^{2-}, NO_3^-, Ca^{2+} and ANC for Cannon Creek that include hindcast and future projections to atmospheric deposition decreases in a) NO_3^- only; b) SO_4^{2-} only; c) Combination of (NO_3^- + SO_4^{2-}). Also shown are measured values.

The Department of the Interior protects and manages the nation's natural resources and cultural heritage; provides scientific and other information about those resources; and honors its special responsibilities to American Indians, Alaska Natives, and affiliated Island Communities.

133/125667, August 2014

National Park Service
U.S. Department of the Interior

Natural Resource Stewardship and Science
1201 Oakridge Drive, Suite 150
Fort Collins, CO 80525

www.nature.nps.gov